Massachusetts Bay Hydrodynamic Model and Water Quality Model results in 1998-99: Comparison Report between HydroQual and University of Massachusetts Boston Runs

Massachusetts Water Resources Authority

Environmental Quality Department
Report ENQUAD 2003-10

Massachusetts Bay Hydrodynamic Model and Water Quality Model results in 1998-99

Comparison Report

between

HydroQual and University of Massachusetts Boston Runs

Dr. Mingshun Jiang

Dr. Meng Zhou

Department of Environmental, Coastal and Ocean Sciences

University of Massachusetts Boston

September 2, 2003

A modeling project
supported by

University of Massachusetts Boston

Massachusetts Water Resources Authority

Citation:

Jiang M and Zhou M. 2003. Massachusetts Bay Hydrodynamic Model and Water Quality Model results in 1998-99: Comparison Report between HydroQual and University of Massachusetts Boston Runs. Boston: Massachusetts Water Resources Authority. Report ENQUAD 2003-10. 42 pp.

TABLE OF CONTENTS

Figure captions

Section 1. Introduction

1.1 Project overview

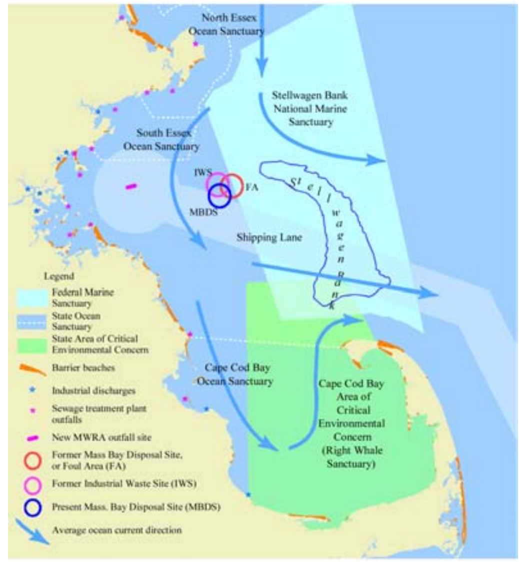

Figure 1.1. Major currents and interest areas in MBS (from Werme and Hunt 2000).

The Massachusetts Bay and Cape Cod Bay system (MBS) is an important economical and recreational area (Figure 1.1), which supports maritime transportation, commercial fishing and other human activities. The Massachusetts Water Resources Authority (MWRA) has funded a number of field and modeling studies to understand the impacts of effluent on the water quality and ecosystem in the MBS since 1980s (Geyer et al., 1992; HydroQual, 2000; HydroQual and Signell, 2001; Libby et al., 1999; Libby et al., 2000; Signell et al., 1996). A long-term Cooperative Research Agreement was made in 2001 between the University of Massachusetts Boston (UMB) and MWRA that the UMB will maintain, enhance and apply the existing Massachusetts Bay Hydrodynamic and Water Quality Models (MB Model), and provide model run results to the MWRA for its obligations under its National Pollutant Discharge Elimination System (NDPES) permit. The hydrodynamic Model (ECOM-si) was developed by the U.S. Geological Survey (USGS) in Woods Hole with assistance from HydroQual Inc. (HydroQual) (Signell et al., 1996). The Water Quality (WQ) Model was developed by HydroQual (HydroQual, 2000). HydroQual had maintained and conducted model runs up to 1999. Under the agreement between the MWRA and HydroQual, the MB model has been transferred to the UMB since 2001. To ensure successful model transfer and consistency between model results produced by different computers and model code setups, a comparison task between UMB and HydroQual model runs has been conducted at the UMB.

The initial task to compare hydrodynamic model results between UMB and HydroQual runs for 1998-1999 was modified because HydroQual delayed their delivery of the 1998-1999 hydrodynamic model run results. To avoid delaying the spinning-up of the MB Model project, the UMB team and MWRA program managers agreed to modify the comparison task by using existing 1994 hydrodynamic model run data instead of using the 1998-1999 runs. The hydrodynamic model comparison was completed in 2002 (Zhou, 2002). The comparison shows that both results are basically identical except the overheated sea surface temperature during several summer days in the HydroQual model run results.

The investigation of the causes for the overheating indicated that the ECOM-si delivered by HydroQual was the latest version with a modified surface heat flux algorithm, which was implemented based on the recommendation from the Model Evaluation Group Committee (MEG). The latest code is more stable. The temperature fields are much smoother without overheating or overcooling the surface layer than those produced by the previous code used in HydroQual runs. This latest code is used by HydroQual for their 1998-99 runs.

The comparison of the WQ Model results between the UMB and HydroQual runs was further delayed due to a number of reasons. Primarily, the MEG requested that the HydroQual WQ Model should use the non-aggregated grids, the same grids used by the hydrodynamic model runs, and a third algal group should be added into the WQ Model to represent the fall phytoplankton assemblage and their bloom. HydroQual delayed their delivery of the 1998-99 MB Model results due to the requested changes in models and codes. The changes in models and codes also diminished the significance of comparing the 1994 WQ model results produced by old models and codes because the future MB Model run will be based on the non-aggregated grids and the revised WQ Models with the third algal group. A new agreement was made between the MWRA program managers and UMB modeling team that the comparison task between the HydroQual and UMB model runs would be made using 1998-99 WQ Model results, and would be delayed till HydroQual delivered their modeling results. Meanwhile, the UMB modeling team has been pursuing 2000-01 hydrodynamic model runs. In February 2003, the HydroQual delivered the first draft of the WQ Model results, the code with the third algal group and the data used to execute the 1998-99 model runs. Then, the comparison task was executed by the UMB modeling team.

1.2 Physical and biological environment

The MBS is approximately 100 km long from north to south, 50 km wide from east to west, and 35 m deep on average. The bay is closed in the north, west and south, and is open to the Gulf of Maine in the east at Stellwagen Bank, which is approximately 20 m deep. Freshwater from Boston Harbor tributaries and the MWRA effluent at the outfall site provide point sources of fresh water and nutrients. Thus, the MBS is a semi-enclosed embayment.

Previous studies have indicated that the circulation in the MBS varies in response to short term and seasonal meteorological forcing, and boundary forcing (Geyer et al., 1992; Signell et al., 1996). The local and remote forces include 1) wind stress and heat fluxes at sea surface, and 2) tides, fresh water runoff and mean surface slopes at open boundaries. The yearly-mean circulation in the MBS is southward and counterclockwise, which is primarily driven by both the intruding current at the northeast corner of the bay associated with mean sea surface slopes, and baroclinic pressure gradients associated with the horizontal density gradients produced by both salinity and temperature differences (Figure 1.2). Tides are dominated by the semi-diurnal M_2 constituent. Tidal currents vary from 10 cm s^{-1} in the interior, to 50 cm s^{-1} off the tip of Cape Cod. The water column stratification varies seasonally. The water column is destratified during late fall, and is mixed in the winter. Stratification occurs in spring due to both freshwater runoff and surface heating. In the summer, the stratification is strongest. The water column is destratified during late fall, and is well mixed in the winter.

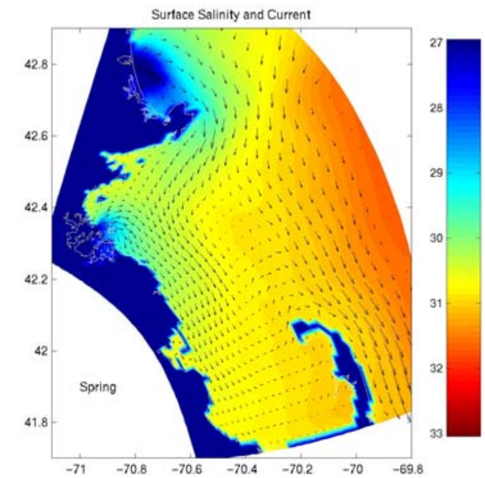

Figure 1.2. Modeled mean surface circulation and salinity in spring.

The surface slope forcing represents the southward flow of the West Maine Coastal Current (WMCC). As early as 1927, Bigelow suggested this current breaks into two branches at Cape Ann; one intrudes deeply into Massachusetts Bay area, and another follows the outer edge of Stellwagen Bank (Figure 1.2) (Bigelow, 1927; Lynch et al., 1996). During spring, the freshwater plume of the Merrimack River interacts with the WMCC, by which the intrusion of WMCC into the MBS is enhanced (Butman, 1976). The main branch of the current remains on the eastern flank of Stellwagen Bank and bypasses the MBS. A branch splits into Massachusetts Bay at Cape Ann, and circulates counterclockwise along the western flank of Stellwagen Bank. This current can intrude into Cape Cod Bay seasonally, especially in winter and spring seasons.

Our recent modeling study indicates pronounced seasonal variation in the circulation pattern. The heating in late spring and summer produces strong horizontal temperature gradients, with warmer water found in Cape Cod Bay area and cooler water in the deep basin near the Stellwagen Bank (Figure 1.3). The temperature gradients are sufficient to block the intruding surface current into Cape Cod Bay in summer and fall. In western Massachusetts Bay, the currents are primarily driven by surface wind: the currents are predominantly southward in the winter-spring season, and northward in the summer and fall. This is confirmed by the moored ADCP (Acoustic Doppler Current Profiler) current measurements at the US Geological Survey buoy.

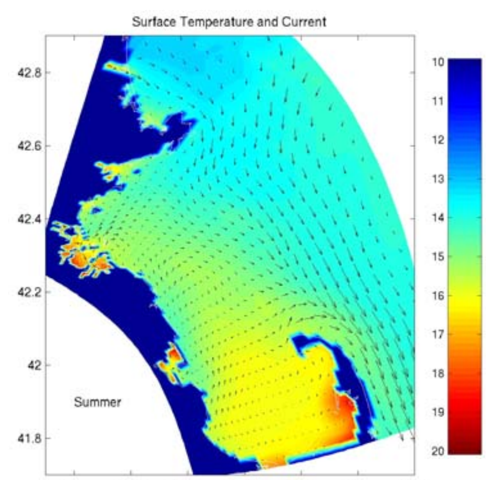

Figure 1.3. Modeled mean surface circulation and temperature in summer.

The reversal of the subtidal current in Massachusetts Bay has significant effects on the dispersion of high nutrient effluent from the MWRA sewage treatment plant. A quick southward transport and dispersion of effluent by the counterclockwise current along the western flank of Stellwagen Bank is expected. The weakening or reversal of the subtidal current near Boston Harbor leads to a longer residence time and weaker dispersion of effluent that could lead to ecological consequences

Phytoplankton growth is primarily driven by nutrient dynamic processes, temperature and photosynthetic available radiation (PAR) (Libby et al., 1999; Libby et al., 2000). The availability of both nitrogen and silica in the well mixed water column during winter leads to the dominance of diatoms in late winter and early spring. The winter and spring bloom is triggered by the warming and increase in solar radiation. The blooms can be episodic and last a few days. In some years, the spring blooms occurred much earlier. The reasons for the earlier spring blooms are not well understood. The onset of stratification limits the upward nutrient fluxes, which in turn limit the primary production in the MBS starting in late spring and early summer. During the summer, the productivity gradually increases, primarily caused by the accumulation of biomass. The abundance of phytoplankton cells reaches its maximum at the end of August. The late summer assemblage is comprised of primarily dinoflagellates and mixed diatoms, mainly the genus *Chaetoceros*. In upwelling areas, the assemblage is dominated by the diatom *Leptocylindrus danicus*. In recent studies, fall phytoplankton blooms were also observed. The fall bloom typically occurs in late September, and declines in November. The bloom is characterized by increases of nutrient concentrations in the surface water and a 2-4 fold increase in diatom abundances.

The biomass of phytoplankton in the MBS supports abundant zooplankton, ranging from 10 to 50×10^3 individuals m^{-3} (Libby et al., 1999; Libby et al., 2000). In winter, zooplankton assemblages were dominated by copepod nauplii, *Oithona similis* females and copepodites, gastropod veligers, and *Acartia hudsonica* females and copepodites. In late winter and early spring, in additional to these mentioned species, subdominant species are bivalve veligers, copepodites of *Calanus finmarchicus*, *Pseudocalanus* and *Temora longicornis*, and *Oikopleura dioica*. In summer and early fall, marine cladoceran *Evadne nordmanni*, *Microsetella norvegica* and copepodites of the genus *Centropages* are added to the species spectrum. In winter, the copepod abundance decreases while the bivalve and gastropod abundances increase.

1.3 Project plan

This comparison report describes the first computational task of this modeling project. The objectives of this task are:

1) to examine the completeness of the MB Model codes delivered by HydroQual,
2) to examine the dependency and independency of these codes on different types of computers, and
3) to give the UMB modeling team an opportunity to learn the codes from the help offered by both

MWRA and HydroQual.

The first objective addresses the completeness of the MB Model. Because the model is developed with hundreds of subroutines, files, data bases, dynamic links between files and variables, and file structures during the last 10-20 years, a test run of the MB Model will identify any missing files which are required for a successful execution of the MB Model. The second objective addresses if the MB Model results produced on different computers under same forcing data are different. For example, the specifics of floating point computations in different computers may lead to an unstable model, or lead to different numerical results. And at last, it is the true test if the UMB modeling team has the capability to understand and execute the MB Model.

The comparison of the hydrodynamic model results between the UMB and HydroQual runs was completed using the 1994 run results. The results indicate that the MB hydrodynamic model produces the consistent results on both HydroQual and UMB computers (Zhou, 2002). The differences between these two runs are the heat flux condition on the sea surface. The UMB is executing the latest version hydrodynamic model with the revised heat flux condition. The results produced by this latest model are nearly identical to those of the earlier version of the model, except those in summer seasons within the surface layer. The current model produces smoother and more stable results in summer within the surface layer than those of the earlier version.

The comparison run of water quality model was conducted by employing the same model codes and data files which were used to produce MB Model results by the HydroQual without any modification, and executing the model run on the UMB computer. After the model run was executed, the results were compared to those in the HydroQual report (HydroQual, 2003).

Section 2. Description of Models

The MB Model consists of a hydrodynamic model and a WQ model. The hydrodynamic model was developed by the USGS at Woods Hole, and calibrated for the period between 1989 and 1994 (Signell et al., 1996) The WQ model, also called the Bays Eutrophication Model (BEM), was developed by HydroQual and calibrated for the period between 1989 and 1991 (HydroQual and Normandeau Assoc., 1995). Though both hydrodynamic and WQ models have been revised since the initial calibration phase, and re-calibrated (HydroQual, 2001b; Zhou, 2002), the basic equations and basic processes remain the same as the original ones.

2.1 Hydrodynamic model

The hydrodynamic model, also called ECOM-si, is based on the primitive equations of mass conservation, momentum balance and Mellor and Yamada level 2-½ turbulence closure (HydroQual, 2000). Both mass conservation and momentum equations include nonlinear advection and vertical turbulence mixing terms. The primitive equations accommodate the nonlinear advection of mass and momentum which is important in shallow water, turbulence mixing induced by both wind stress and bottom friction, baroclinic currents induced by horizontal density gradients and barotropic currents produced by surface slopes. Thus, the modeling results of ECOMsi in Massachusetts Bay include tide, tidal currents, baroclinic currents driven by horizontal density gradients, and stratification produced by fresh water runoff and surface heat flux. A detailed description of ECOMsi can be found in the HydroQual report (HydroQual, 2000).

The ECOMsi is based on the primitive equations of motion. The continuity equation is:

$$\frac{\partial \eta}{\partial t} + \frac{\partial (uD)}{\partial x} + \frac{\partial (vD)}{\partial y} + \frac{\partial w}{\partial \sigma} = 0\,, \tag{2-1}$$

where η is the surface elevation, x and y represent 2 independent horizontal axes, z is the vertical axis, u, v and w are the velocity components in x, y and z directions, D is the total water depth, and σ is the normalized vertical coordinate defined as

$$\sigma = \frac{z - \eta}{H + \eta}, \tag{2-2}$$

where H is the depth of water column. The momentum equations are:

$$\frac{\partial uD}{\partial t}+\frac{\partial(u^2D)}{\partial x}+\frac{\partial(uvD)}{\partial y}+\frac{\partial(uw)}{\partial\sigma}-fvD=$$

$$-gD\frac{\partial\eta}{\partial x}+\frac{\partial}{\partial\sigma}\left(\frac{K_M}{D}\frac{\partial u}{\partial\sigma}\right)-\frac{gD^2}{\rho_0}\frac{\partial}{\partial x}\int_\sigma^0\rho d\sigma+\frac{gD}{\rho_0}\frac{\partial D}{\partial x}\int_\sigma^0\sigma\frac{\partial\rho}{\partial\sigma}d\sigma+F_x\ , \tag{2-3}$$

$$\frac{\partial vD}{\partial t}+\frac{\partial(uvD)}{\partial x}+\frac{\partial(v^2D)}{\partial y}+\frac{\partial(vw)}{\partial\sigma}+fuD=$$

$$-gD\frac{\partial\eta}{\partial y}+\frac{\partial}{\partial\sigma}\left(\frac{K_M}{D}\frac{\partial v}{\partial\sigma}\right)-\frac{gD^2}{\rho_0}\frac{\partial}{\partial y}\int_\sigma^0\rho d\sigma+\frac{gD}{\rho_0}\frac{\partial D}{\partial y}\int_\sigma^0\sigma\frac{\partial\rho}{\partial\sigma}d\sigma+F_y\ , \tag{2-4}$$

where g is the gravity, f is the Coriolis constant, K_M is the vertical turbulence mixing coefficient, ρ is the density of water, ρ_0 is the mean density, and F_x and F_y are horizontal mixing coefficients in x and y directions. The horizontal mixing coefficients can be parameterized as

$$F_x=\frac{\partial}{\partial x}\left(2A_MD\frac{\partial u}{\partial x}\right)+\frac{\partial}{\partial x}\left[A_MD\left(\frac{\partial u}{\partial y}+\frac{\partial v}{\partial x}\right)\right], \tag{2-5}$$

$$F_y=\frac{\partial}{\partial y}\left[A_MD\left(\frac{\partial u}{\partial y}+\frac{\partial v}{\partial x}\right)\right]+\frac{\partial}{\partial y}\left(2A_MD\frac{\partial v}{\partial y}\right), \tag{2-6}$$

where A_M is the turbulent horizontal eddy mixing coefficient.

The vertical turbulence mixing is estimated by using Mellor and Yamada's level 2-½ turbulence closure with the extensions by Galperin et al. (1988). The extension prevents the mixing length from being overestimated in the stratified condition. The background mixing value is set to the molecular viscosity of 5×10^{-2} cm^2 s^{-1}. Because of the positive definite semi-implicit finite difference scheme, the numerical diffusivity overtakes the molecular viscosity.

The bottom boundary condition is given by the estimate of bottom stresses based on the logarithmic law (or constant stress layer). The key parameter, the bottom roughness z_0, is estimated based on the best-fit to tides in Massachusetts Bay. For the future, this value should be objectively estimated from the tidal energy balance.

The surface heat flux is calculated based on formulae used in previous modeling studies in Massachusetts Bay (Signell, 1996). In the model, the heat flux is contributed by precipitation, evaporation, short wave radiation, long wave radiation, and sensible heat. The wind stress is calculated from wind speed and direction measured at the Boston Buoy using the Large and Pond formulation (Large and Pond, 1981).

2.2 Water quality model

The WQ Model includes basic biochemical-primary production processes in the water column and bio-geochemical processes in sediments. The revised WQ Model considers winter, summer and fall algal groups. These three groups represent different assemblages of phytoplankton species. The distinctions are made to recognize the differences in the physiological rates in terms of optimal temperature and light conditions and nutrient requirements. The kinetic framework used for these functional groups is the same (Laws and Chalup, 1990; Shuter, 1979), i.e.,

$$G_p = \mu_{P\max}(T_{opt})\ G_T(T)\ G_I(I)\ G_N(N), \qquad (2\text{-}7)$$

where G_P is the growth rate, $\mu_{P\max}$ is the nutrient saturated growth rate at the optical temperature and light, G_T is the reduction factor caused by temperature, G_I is the reduction factor caused by light attenuation, and G_N is the reduction factor caused by nutrient limitation. The nutrients used in the model include nitrogen, phosphorus and silica. The Michaelis-Menten expression is used for each nutrient and the minimum value is chosen to reduce the saturated growth rate,

$$G_N = Min\left(\frac{\mathrm{DIN}}{\mathrm{K_{mN}} + \mathrm{DIN}}, \frac{\mathrm{PO_4}}{\mathrm{K_{mP}} + \mathrm{PO_4}}, \frac{\mathrm{DSi}}{\mathrm{K_{mSi}} + \mathrm{DSi}}\right), \qquad (2\text{-}8)$$

where DIN is the concentration of dissolved inorganic nitrogen , PO_4 is the total dissolved phosphorus, and DSi is the total dissolved silica. K_{mN}, K_{mP} and K_{mSi} are the Michaelis or half-saturation constants for nitrogen, phosphorus and silica. The nutrient assimilation rate is constrained by

$$\frac{d}{dt}(S + L + D) = W_{Cx} f_N, \qquad (2\text{-}9)$$

where S is the structural carbon, L is the light-reaction carbon, D is the dark-reaction carbon, W_{Cx} is the ratio of carbon to a given nutrient and f_N is the rate of nutrient assimilation. The total carbon C is equal to

$$C = S + R + L + D, \qquad (2\text{-}10)$$

where R is the reservoir carbon. The rate of change in the total carbon is

$$\frac{dC}{dt} = G_{\Pr L} LI - k_{RB} R - k_{RG} G_{\Pr L} LI, \qquad (2\text{-}11)$$

where G_{PrL} is the daily gross rate of photosynthesis per unit L per unit I, k_{RB} is the daily respiration rate to maintain the cell, and k_{RB} is the daily growth-dependent respiration rate. If we take the format of the carbon specific growth rate, μ,

$$\mu C = G_{\Pr L} LI - k_{RB} R - k_{RG} G_{\Pr L} LI, \qquad (2\text{-}12)$$

we have the nutrient saturated condition,

$$\mu_{P\max} = \frac{G_{\Pr d}(1-k_{RG})(1-S/C)I}{I + G_{\Pr d}/G_{\Pr Ls}} - k_{RB}\frac{R}{C}, \qquad (2\text{-}13)$$

where G_{PrLs} is the nutrient-saturated value of G_{PrL}..

The grazing of both micro and mesozooplankton is parameterized simply by

$$k_{grz} = k_{grz}(20^{\circ}C)\theta_{rz}^{(T-20)} \qquad (2\text{-}14)$$

where k_{grz} is the temperature corrected loss rate due to zooplankton grazing and θ_{grz} is the temperature correction factor for zooplankton grazing (See section 4.3 for discussions of this simplification.)

The uptake of nutrients by phytoplankton is calculated from the ratio of a nutrient to the carbon (N_x/C) in cells,

$$\frac{d}{dt}\left(\frac{N_x}{C}\right) = k_{eq}\left[\left(\frac{N_x}{C}\right)_{eq} - \left(\frac{N_x}{C}\right)\right] \qquad (2\text{-}15)$$

where $(N_x/C)_{\mathrm{eq}}$ is the ratio of a nutrient to carbon at equilibrium, and k_{eq} is the rate to achieve equilibrium. Chlorophyll is calculated in the same way using the equilibrium ratio of the chlorophyll to carbon $(Chl/C)_{\mathrm{eq}}$ in cells,

$$\frac{d}{dt}\left(\frac{Chl}{C}\right) = k_{eq}\left[\left(\frac{Chl}{C}\right)_{eq} - \left(\frac{Chl}{C}\right)\right] \qquad (2\text{-}16)$$

Equations 2-7 and 2-16 explicitly express the biological and biochemical processes associated with phytoplankton. The nutrients, carbons and other biochemical constituents in the water column are calculated from the conservation equations including advection-mixing processes and rates of sources and sinks. The details of equations and parameters for all constituents in the water column can be found in HydroQual and Normandeau Assoc.(1995) and HydroQual (2001b).

2.3 Sediment model

The sediment model consists of two layers, the aerobic and anaerobic layers (DiToro and Fitzpatrick, 1993). In these two layers, we assume four separate processes: 1) downward fluxes of particulate organic matter (POM) from the overlying water column to the sediments, 2) diagenesis converting POM to soluble intermediates, 3) reactions converting a portion of the soluble species into particulate species, and 4) diffusion fluxes of these species into the water column overlying the sediment. Because the diagenesis and reactions in sediments require oxygen, the oxygen supplies from the overlying water limit the production of these processes. The diffusion flux of dissolved oxygen (DO) through the interface between the overlying water column and sediment can be written as

$$SOD = D_1 \frac{O_2(\text{overlying water})}{H_1} \tag{2-17}$$

where D_1 is the diffusion coefficient in the aerobic layer, H_1 is the thickness of the aerobic layer, and SOD is the sediment oxygen demand for balancing the nitrification processes in the aerobic layer. Equation 2-17 should also serve the bottom boundary condition of the DO in the water column. The SOD can be further calculated from the oxygen consumption due to processes of diagenesis and reactions driven by the particular organic matter (POM) in the aerobic layer.

The flux of POM is determined by the biomass of phytoplankton and detritus and specified settling velocities in the water column overlying the sediment. The diagenesis of POM, reactions and productions of nutrients and DO are calculated from the mass balance equations and Monod kinetics (Di Toro and Fitzpatrick, 1993; HydroQual and Normandeau Assoc., 1995). The soluble nutrients in sediments will then be transferred into the overlying water column.

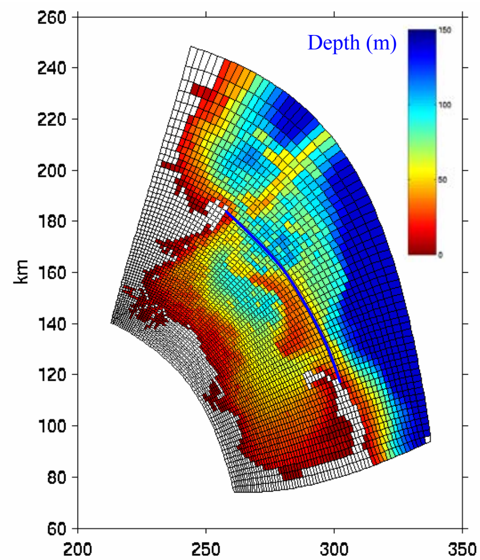

Figure 2.1. The model grids and bathymetry. The blue solid line in the figure indicates the BEM model domain.

2.4 Model geometry and bathymetry

The hydrodynamics model is configured on 68×68 horizontal curvilinear orthogonal grids (Figure 2.1). The grid spacing varies from approximately 600 m in Boston Harbor to approximately 6 km at the open boundary. There are 12 sigma levels in the vertical, varying from 1%, 4% and 5% of the local water column depth for the top 3 layers, to 10% for the remaining 9 layers.

The National Ocean and Atmospheric Administration (NOAA) sounding data are used to determine the bathymetry at each grid point. To reduce noises in the model fields, the depths used in the model are smoothed by applying the Shapiro filter to remove 2-grid length variability (Shapiro, 1975). To avoid flooding and drying in modeling segments, the minimum depth is set to be 3 m, and to eliminate the complication of sharp topography in offshore areas, the maximum depth is set to be 140 m.

The BEM model is configured on the "full grids" in the horizontal, the same grids in a reduced model domain from Cape Ann to Provincetown indicated by the blue solid line in Fig. 2-1. The vertical configuration is same as the hydrodynamic model.

2.5 Boundary and initial conditions

Boundary conditions of elevation, temperature and salinity are required at the open boundaries of the modeling area for the hydrodynamic model. The boundary condition for elevation incorporates the mean surface slope and tidal constituents as the forcing parameters, while surface gravity waves can freely pass through. The boundary condition applied in the model is a partially specified and partial radiation boundary condition (Blumberg and Kantha, 1985), i.e.

$$\frac{\partial \eta}{\partial t} + \sqrt{gD}\,\frac{\partial \eta}{\partial x} = \frac{\eta - \eta_{data}}{T_{lag}} \tag{2-18}$$

where η_{data} is the given force, and T_{lag} is the relaxation time. Equation (2-18) will reduce to a pure radiation boundary condition when T_{lag} is larger than the period of gravity waves, and Equation (2-18) will be reduced to a specified boundary condition when T_{lag} is less than the period of gravity waves. The choice of T_{lag} is empirical. At the northern portion of the open boundary, a specified boundary condition is applied representing the forcing from the Gulf of Maine, and at the southern portion, a radiation boundary condition is applied to allow the reflected gravity waves pass out the computational region.

The temperature and salinity are specified or calculated along the open boundaries. The boundary values are specified using a fixed value for inflow, and calculated from the advection condition for the outflow. A description of how to estimate boundary condition values can be found in (HydroQual, 2001a).

The WQ model requires boundary conditions of nutrient and chlorophyll concentrations at the open boundaries of the modeling area. The nutrient values in the deep water are used based on historic data which have relatively small variability, and the values in the surface water are interpolated or extrapolated from measurements obtained in the "Far-field" surveys. Chlorophyll concentrations at the open boundaries are set to zero. From the sensitivity analysis of open boundary conditions, results indicate that the chlorophyll biomass in MBS is primarily determined by the productivity in the bay (HydroQual., 2001a). The import and export of chlorophyll biomass are negligible.

The initial conditions for the 1998-99 circulation modeling runs were provided by HydroQual as a part of the model package. Typically there are two initialization methods used by HydroQual: 1) currents are set to be zero over the modeling area, and temperature and salinity are set using observational data; or 2) the current, temperature and salinity fields are set using modeling results. In the first case, the initial period of modeling results may suffer the limited availability of observation data for the setting of initial conditions. After this initial period, the physical fields are determined by boundary conditions imposed at the open boundaries and surface. In the second method, it requires the computation of physical fields for each year. The HydroQual hydrodynamic modeling is initialized from year 1989. Using existing simulation data to initialize the model and compare our modeling results to existing modeling data should be the best way to test the consistency of the same model running on different computers.

The boundary conditions at open boundaries and surface were provided by HydroQual, which should be in the same format as those used in their modeling for 1994.

Section 3. Comparisons between HydroQual and UMass model results

3.1 Model runs

The UMass WQ model is based on three algal groups because the three-algal group model is recommended by the MEG for the future water quality modeling in the MBS. We used exactly the same model setups, model parameters and model forcing as those used by HydroQual though an error in the MWRA Nut Island flow data was discovered (some flow through the Nut Island outfall had been added to Deer Island flow) after the model run was finished by HydroQual. Only for the comparison purpose, we used the same flows and loads as those in the HydroQual 1998-99 water quality run report (HydroQual, 2001b; HydroQual, 2003). A simulation using corrected flows and loads could be conducted in the future.

Several changes were made during execution of the UMass WQ model because of the machine dependences on the binary data formats and dealing with zeros. Initially, efforts to use binary data provided by HydroQual were made in the UMass run. However, there is a difference in the binary formats between SGI and DEC workstations. The UMass WQ could not read the binary initial condition data successfully. The binary initial condition was converted to ASCII data with help from HydroQual. During the data conversion, the precision or the number of significant digits of binary data is different from the ASCII that is machine-dependent on the floating point treatment.

A few division-by-zero errors occurred during execution, and were fixed; most of these were either at grids on land or cases of zero divided by another zero. These divisions were set to zero in the UMass run based on known physical-biochemical processes. There is a lack of information how a SGI workstation deals with such division-by-zero errors. Typically, a random small number would be assigned automatically. We expect that though floating point corrections may cause small fluctuations in the model results, the corrections should not have significant effects on the model results if the model is inherently stable. The model was executed successfully after these changes.

3.2 Comparison

We chose variables for the comparison based on:

1) those variables used in the HydroQual report (HydroQual, 2001b; HydroQual, 2003),

2) the loadings and end products in a chain of reactions, and

3) those used for environmental indexes.

The temporal comparison is made using time series at the surface and bottom at selected stations (Figure 3.1) which are used in the HydroQual report. In additional to these time series, horizontal maps of selected variables are used to show the spatial comparison between the UMass and HydroQual results. The variables used are listed in Table 1. We believe that these variables can reflect most of the important features and details in the model results. For the simplicity and the detailed features in illustrated figures, we also chose results only in 1998. From the comparison, we can simply apply the conclusions from the 1998 results to the 1999 results.

Table 1

Water Column	**Sediment**
chlorophyll	POC
particular organic carbon (POC)	POC flux
dissolved inorganic nitrogen (DIN)	sediment oxygen demand (SOD)
silicate (Si)	nitrate flux (JNO_3)
bottom dissolved oxygen (DO)	silicate flux (JSi)
primary production	

3.2.1 Time series comparison in water column

The temporal comparison of surface chlorophyll between UMass and HydroQual results in 1998 is shown in Figure 3.2. The general trends are exactly same at all six selected stations though some small secondary differences can be found at a time scale of 4-5 days. The exact reasons for these differences have not been understood though several trials were made. The differences can come from several sources: the differences in the machine-dependent floating point treatments and the numerical filters used by UMass and HydroQual. Because the differences are so small and within the accuracy of a numerical model, we conclude that the results from UMass and HydroQual are fundamentally the same. The same conclusion can be applied to other variables: the surface DIN (Figure 3.4), surface Si (Figure 3.5), bottom DO (Figure 3.6), vertically integrated primary production (Figure 3.7), NO_3 flux (Figure 3.8), SOD (Figure 3.9) and Si flux (Figure 3.10).

The differences of DIN and Si between UMass and HydroQual results are relatively large during the initial period, compared to those after a month (Figures 3.4 and 3.5). Because biological activity in winter period is very low, the initial differences of DIN and Si are likely brought into from the initial conditions and remain by mass conservation. The spatial and temporal changes of DIN and Si are determined by advection and diffusion processes in the initial period.

The differences of DIN and Si diminish when biological activity enhances in spring. The differences of DIN and Si are transferred into chlorophyll, POC and DO through biological activity. Then the differences appear in those variables within the sediment. Finally, all differences diminish in late fall and winter. These processes demonstrate the possible error sources, and dissipation of these errors. The convergence between UMass and HydroQual results indicates the robustness of this WQ model and the sensitivity of this model to the initial conditions.

3.2.2 Horizontal field comparison in water column

The spatial comparison of mean surface chlorophyll in the spring season (March through May) between UMass and HydroQual results is shown in Figure 3.11. No difference between these two surface maps of chlorophyll can be identified visually. The difference can only be inspected from detailed time series at a chosen location such as shown in Figure 3.2. The comparison of mean surface DIN and bottom DO in spring yields the same conclusion (Figures 3.12 and 3.13).

The differences in time series between UMass and HydroQual results can be carefully examined in snap shots of surface chlorophyll, surface DIN and bottom DO between April 29 and May 3 though they are nearly identical (Figures 3.14, 3.15 and 3.16). The surface chlorophyll shows that the concentration near Deer Island from the UMass result is higher than that of the HydroQual result (Figure 3.14), which is coincident with a high DIN tongue and slightly low DO extending from Deer Island in the UMass result (Figures 3.15 and 3.16). As we discussed, these differences result from the initial conditions.

The close agreement between these two model results in both time and space demonstrate that a small error introduced at a given time and location will not be amplified after the long time integration.

3.2.3 Horizontal field comparison in sediment

The estimates of annual mean POC in sediment from these two model results also show no difference (Figure 3.17). Because annual POC is accumulative, the comparison of annual mean POC indicates that there is no accumulative error or difference between these two model results. The same conclusion can be applied to the annual mean flux of POC to sediments (Figure 3.18). It is also apparent that the differences between UMass and HydroQual results are larger for variables within the water column than those in the sediment.

3.3 Conclusions

1) The WQ model produces the same results on different computers.

2) The model is robust to the perturbation in initial conditions and produced during the integration process, i.e., the errors in variables will be dissipated.

3) The sediment model is less sensitive to the treatment of floating points or correction of overflow due to zero division.

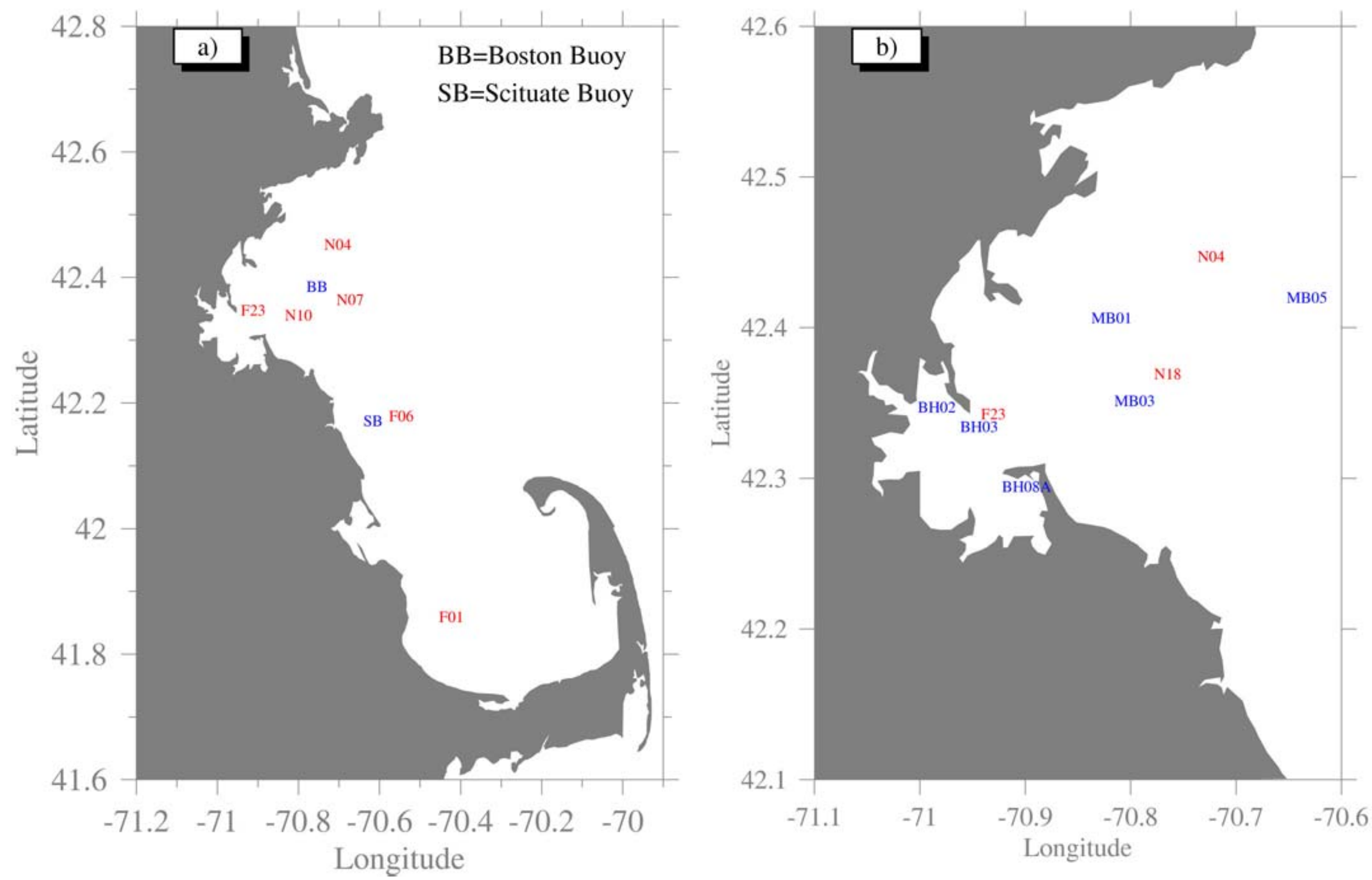

Figure 3.1. Locations of time series stations for comparisons: a) stations used for comparisons in water column, b) stations used for sediment fluxes (blue) and primary production (red).

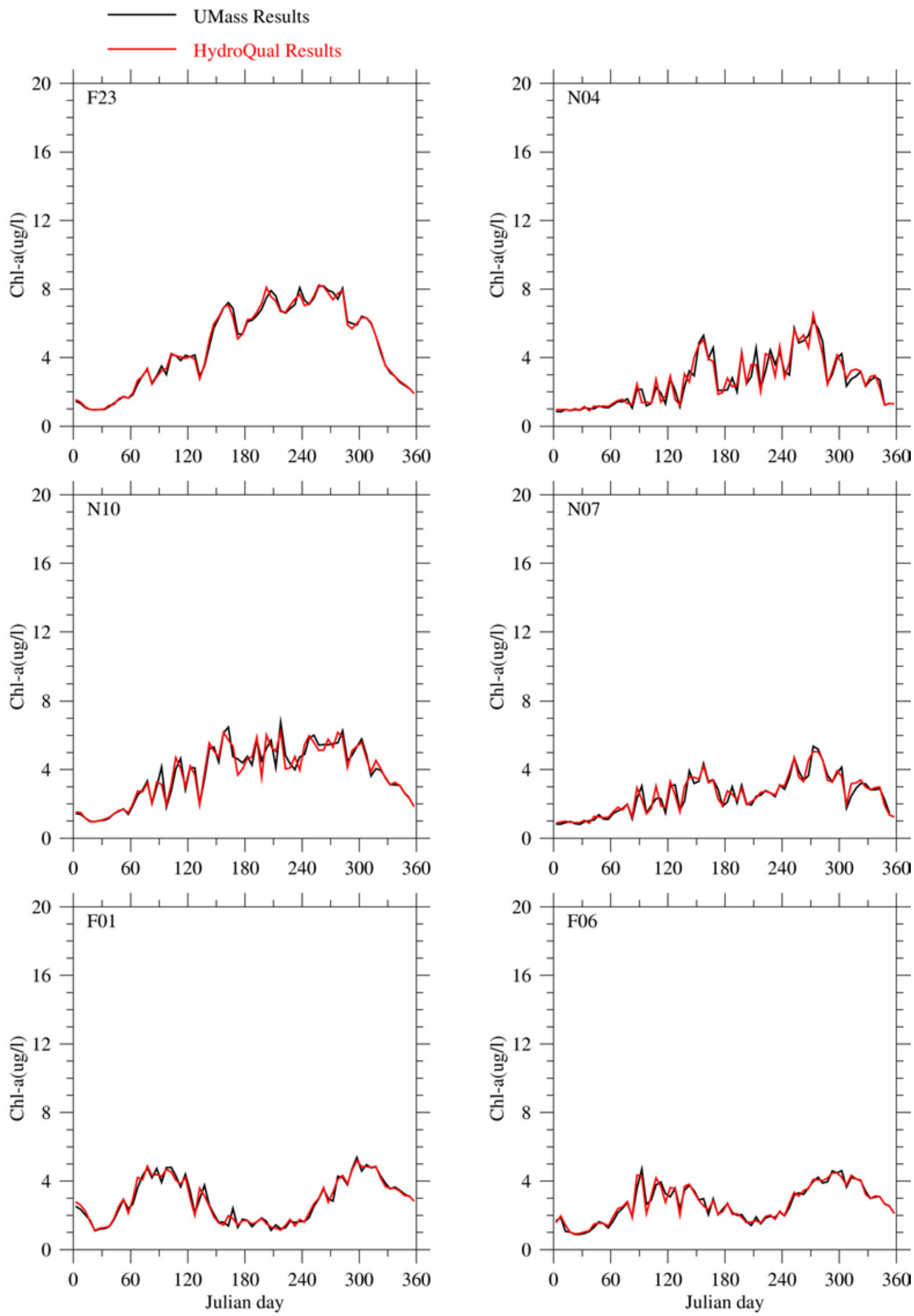

Figure 3.2. Surface chlorophyll concentrations

at selected stations.

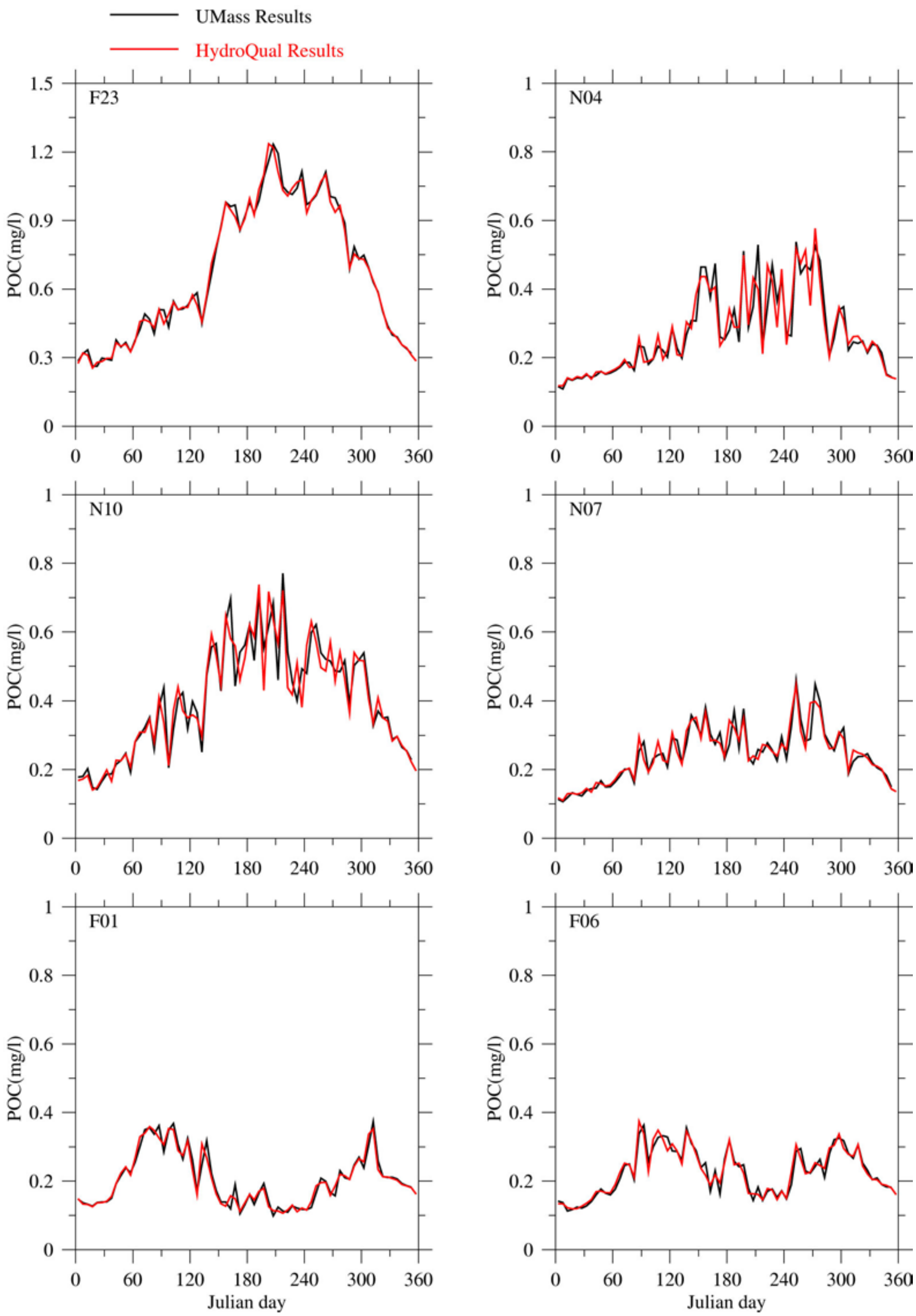

Figure 3.3. Surface total POC concentrations at selected stations.

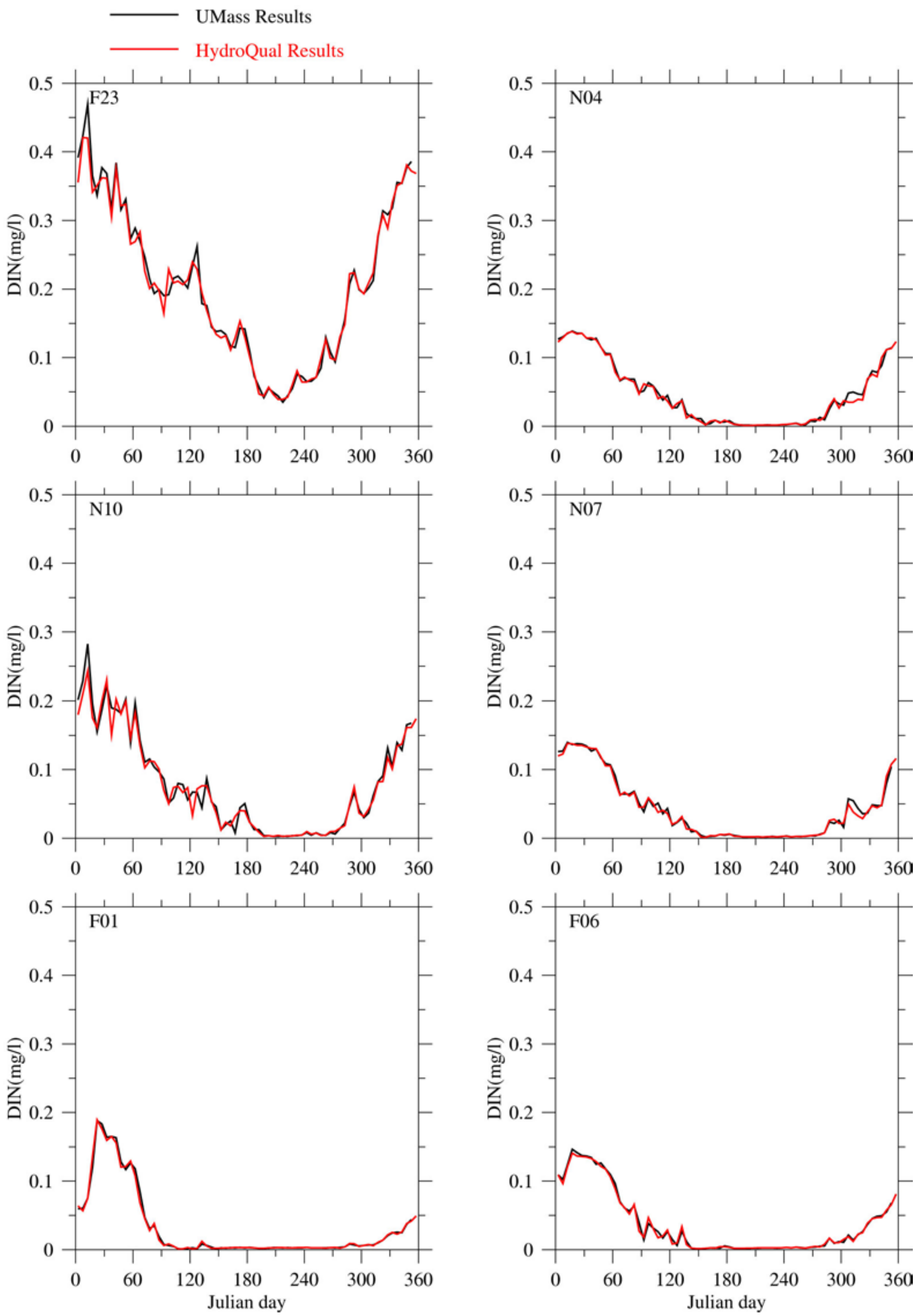

Figure 3.4. Surface DIN concentrations at selected stations.

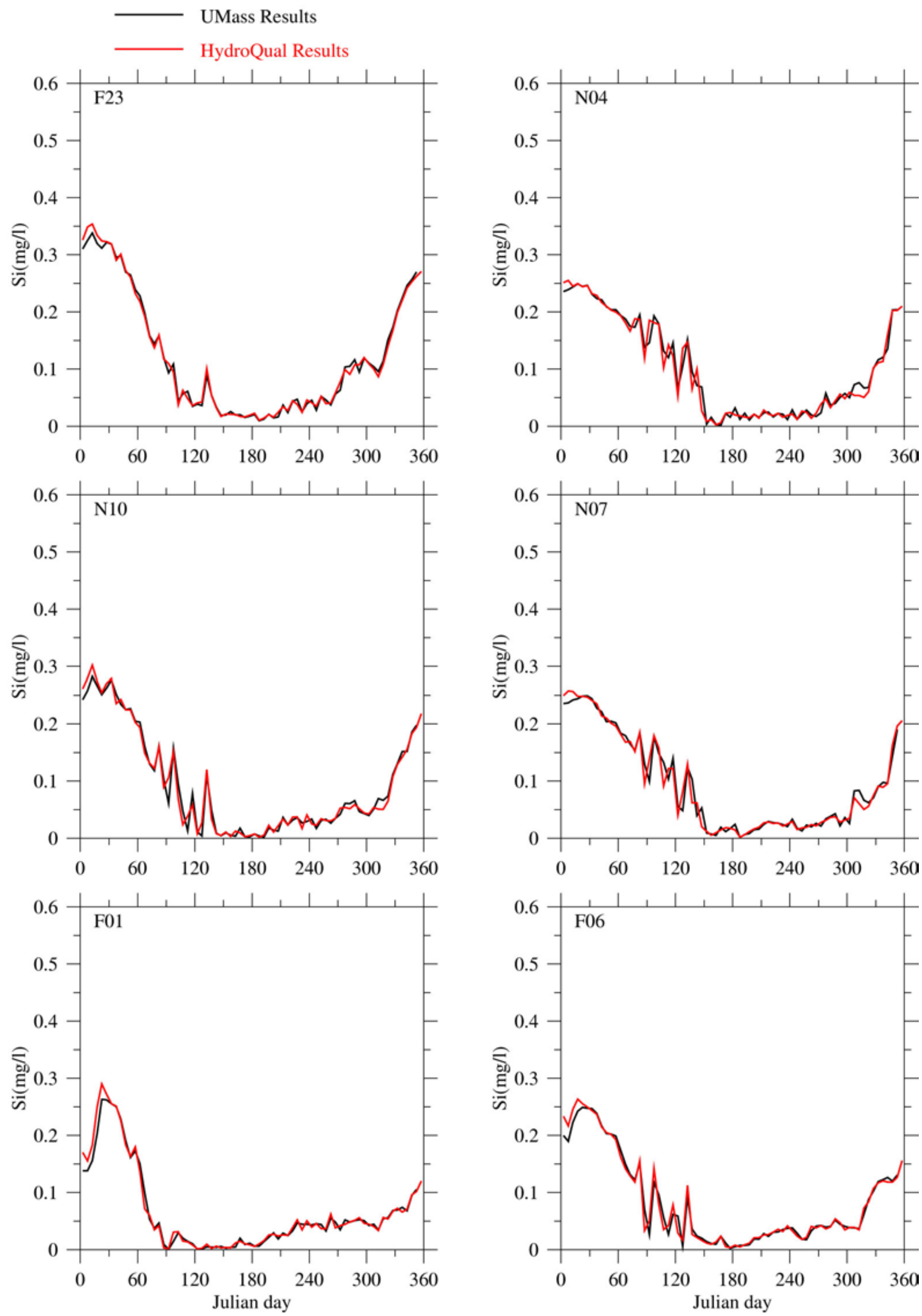

Figure 3.5. Surface Si concentrations at selected stations.

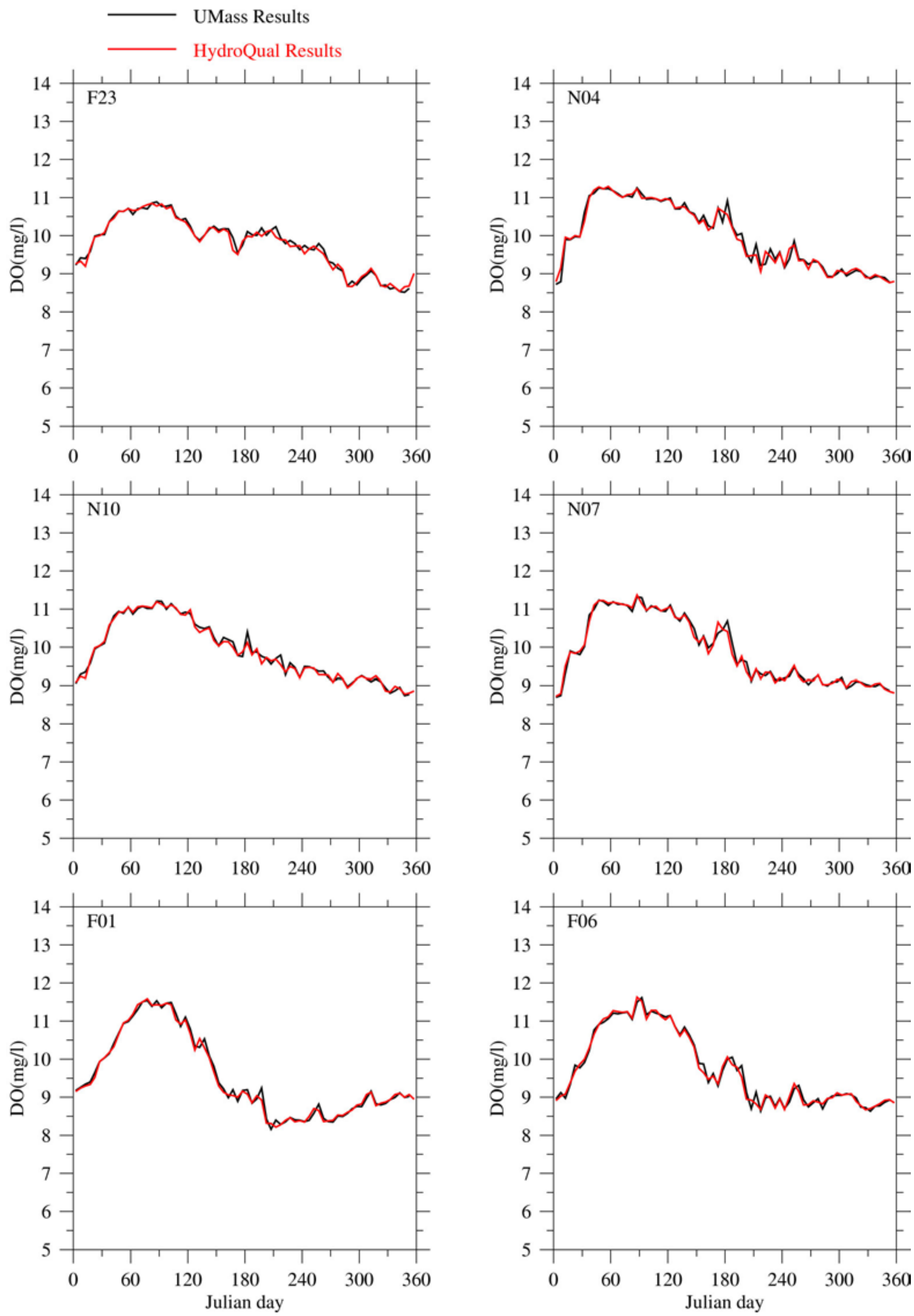

Figure 3.6. Bottom DO concentrations at selected stations.

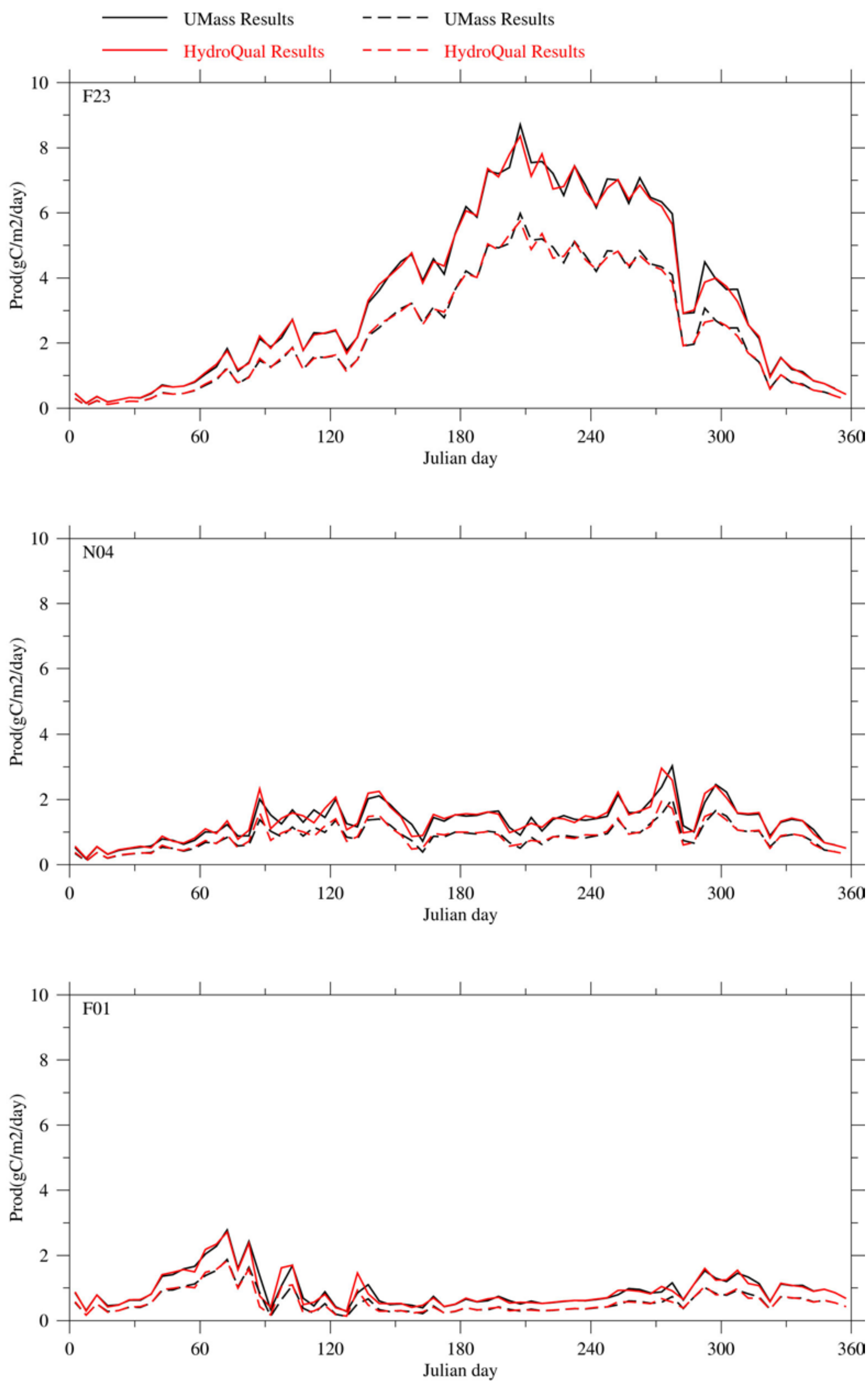

Figure 3.7. Primary productivity at selected stations (Solid lines: gross primary productivity, dashed lines: net primary productivity)

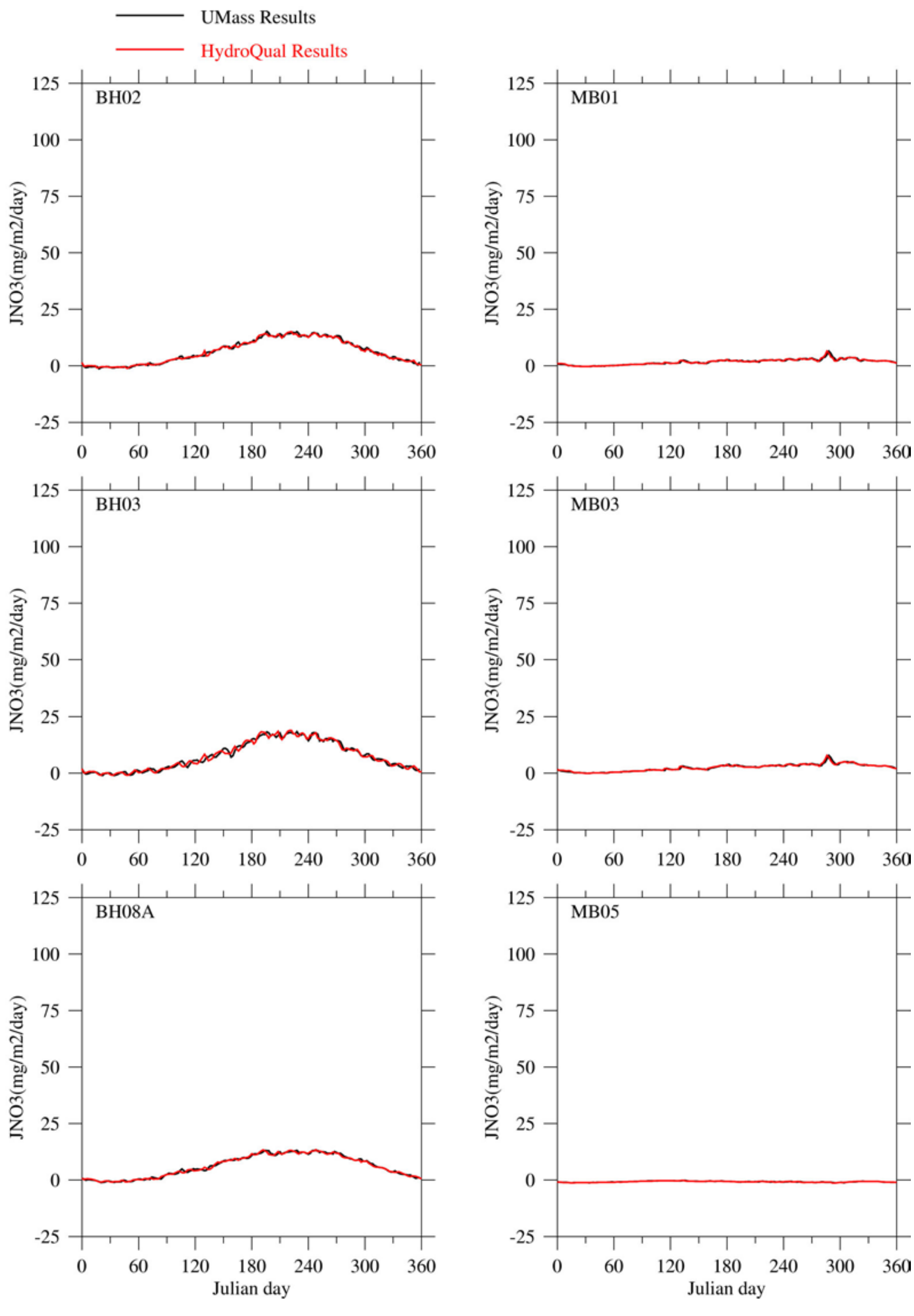

Figure 3.8. Nitrate flux from the sediment at selected stations.

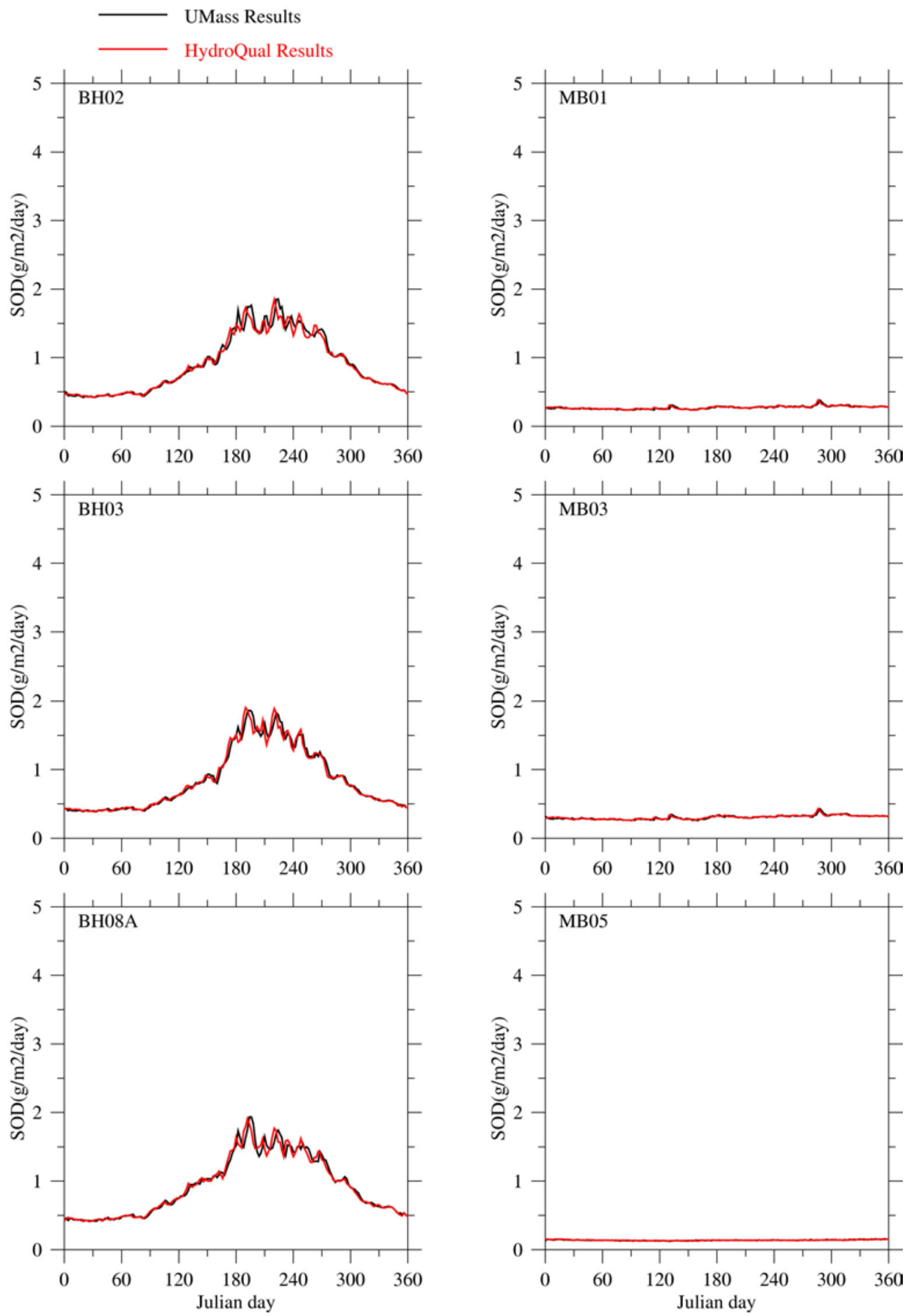

Figure 3.9. Sediment oxygen demand (SOD) at selected stations.

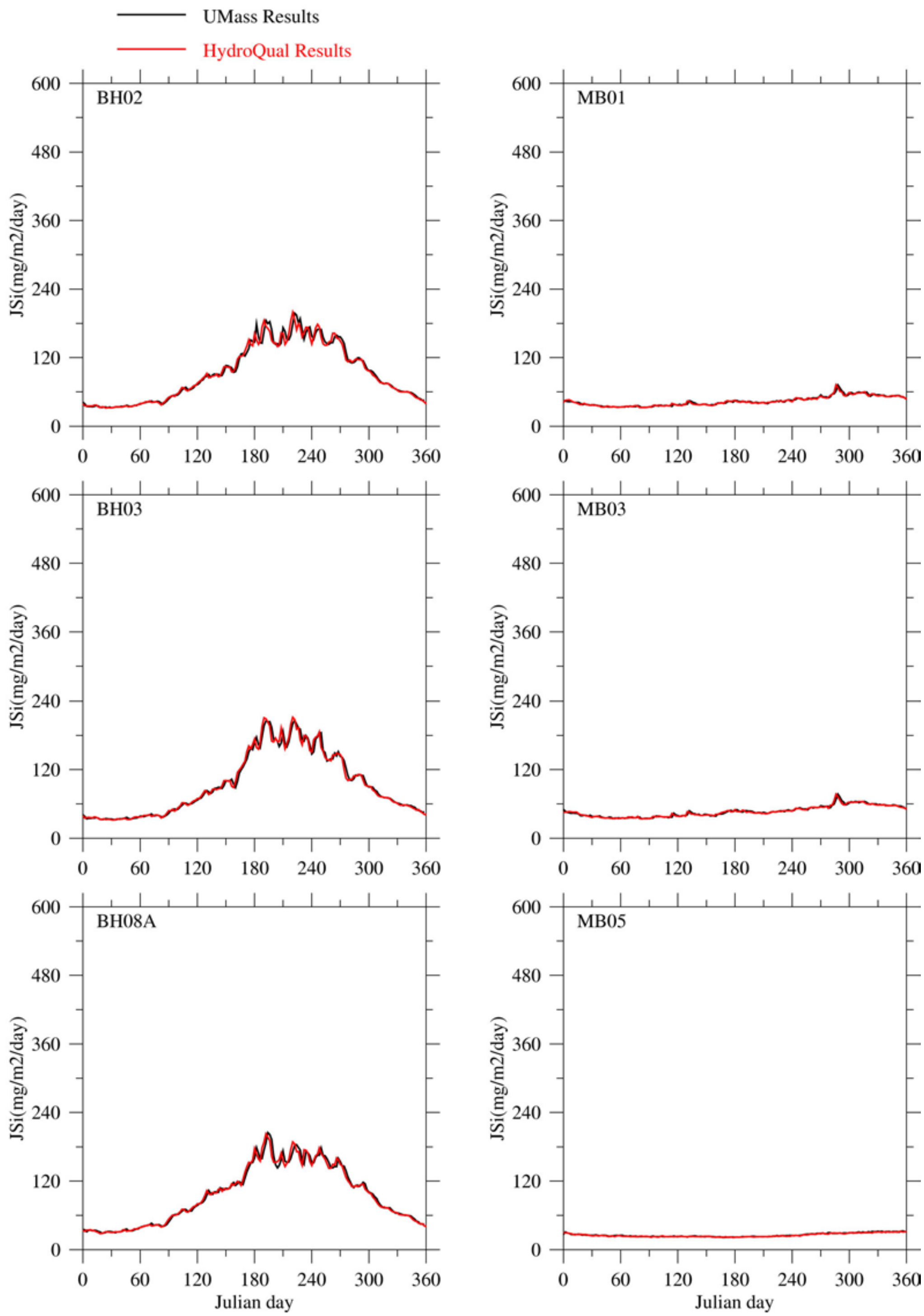

Figure 3.10. Silicate flux from sediment at selected stations.

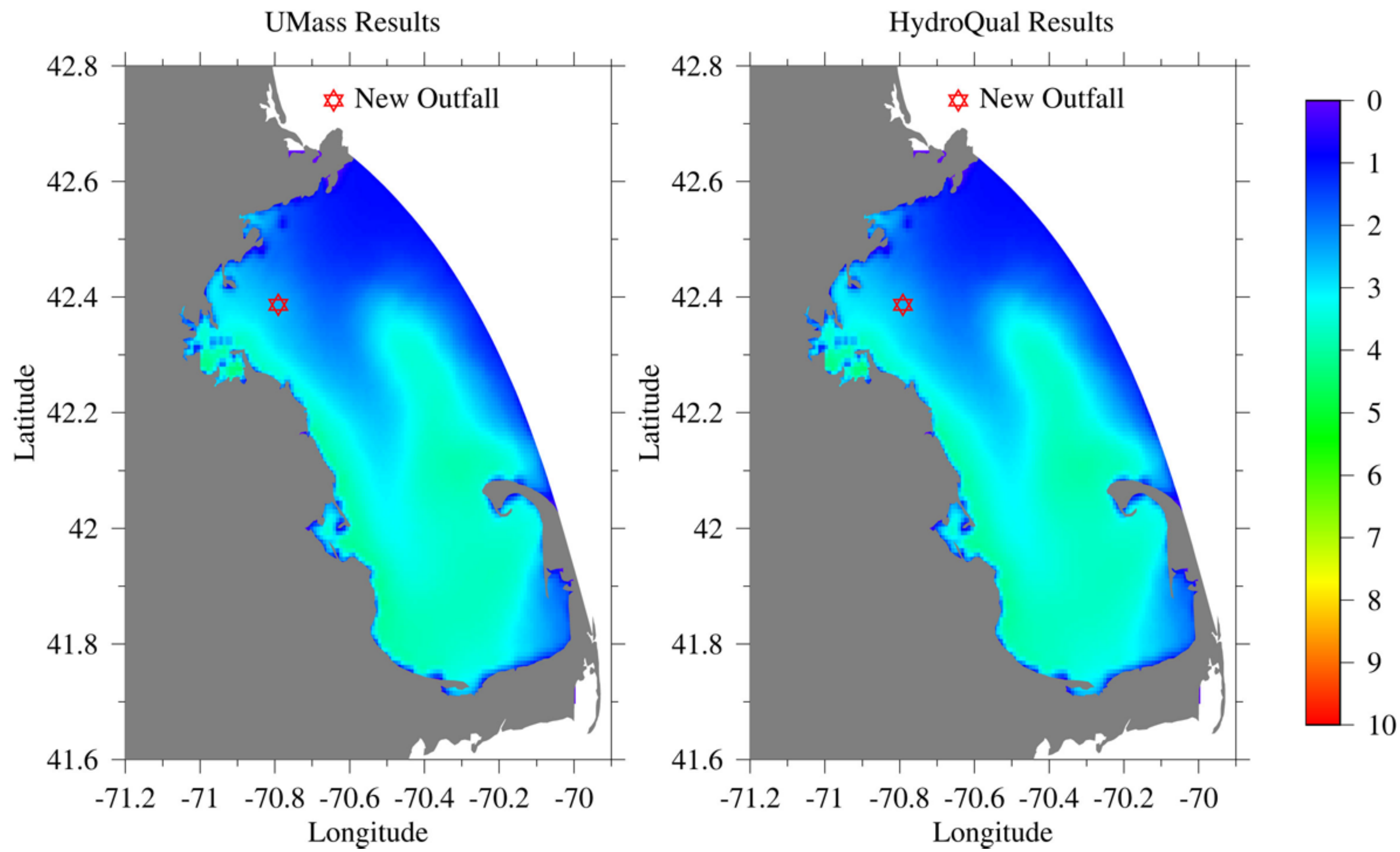

Figure 3.11. Surface Chlorophyll concentrations in spring (March-May).

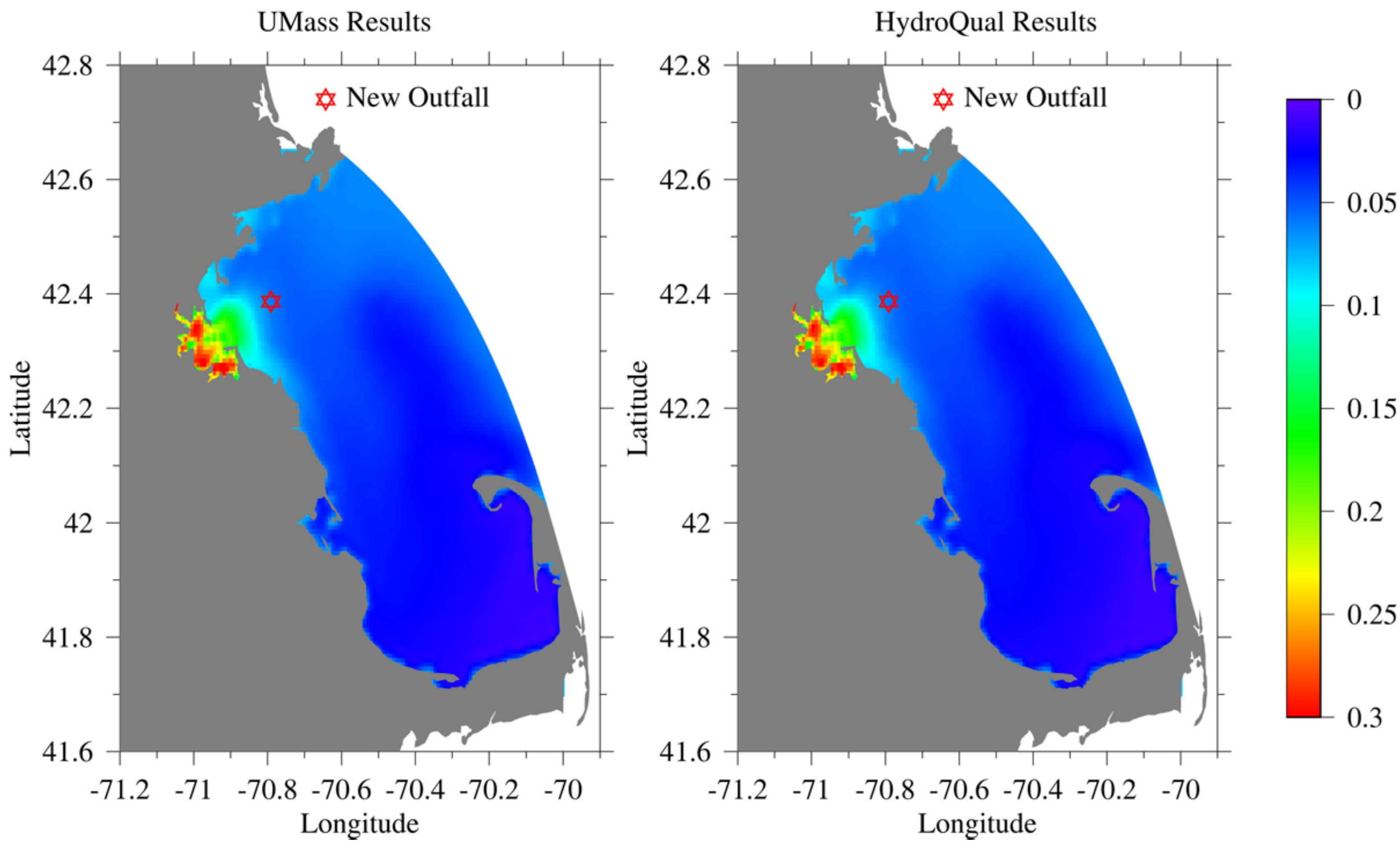

Figure 3.12. Surface DIN concentrations in spring (March-May)

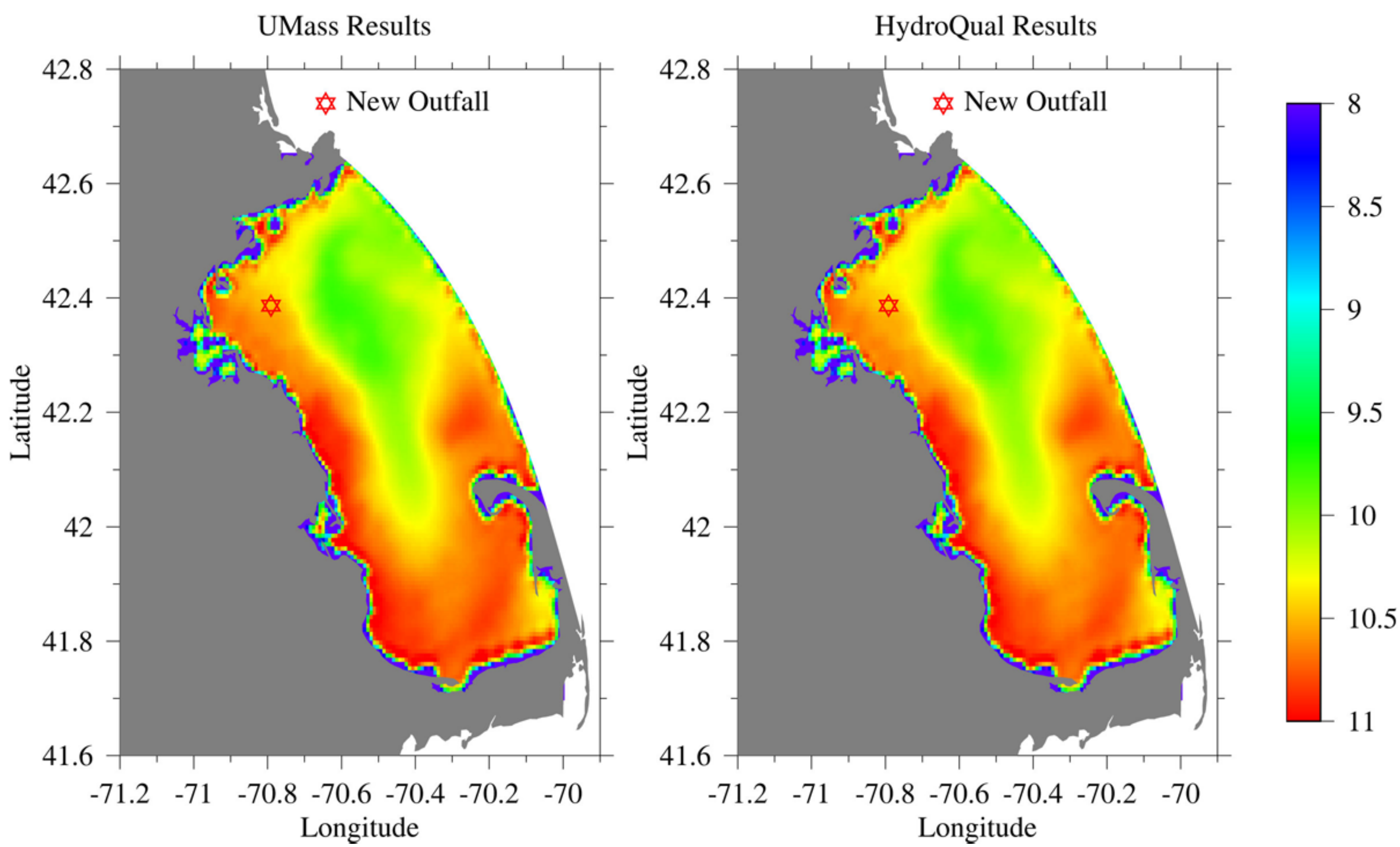

Figure 3.13. Bottom dissolved oxygen (DO) concentrations in spring (March-May)

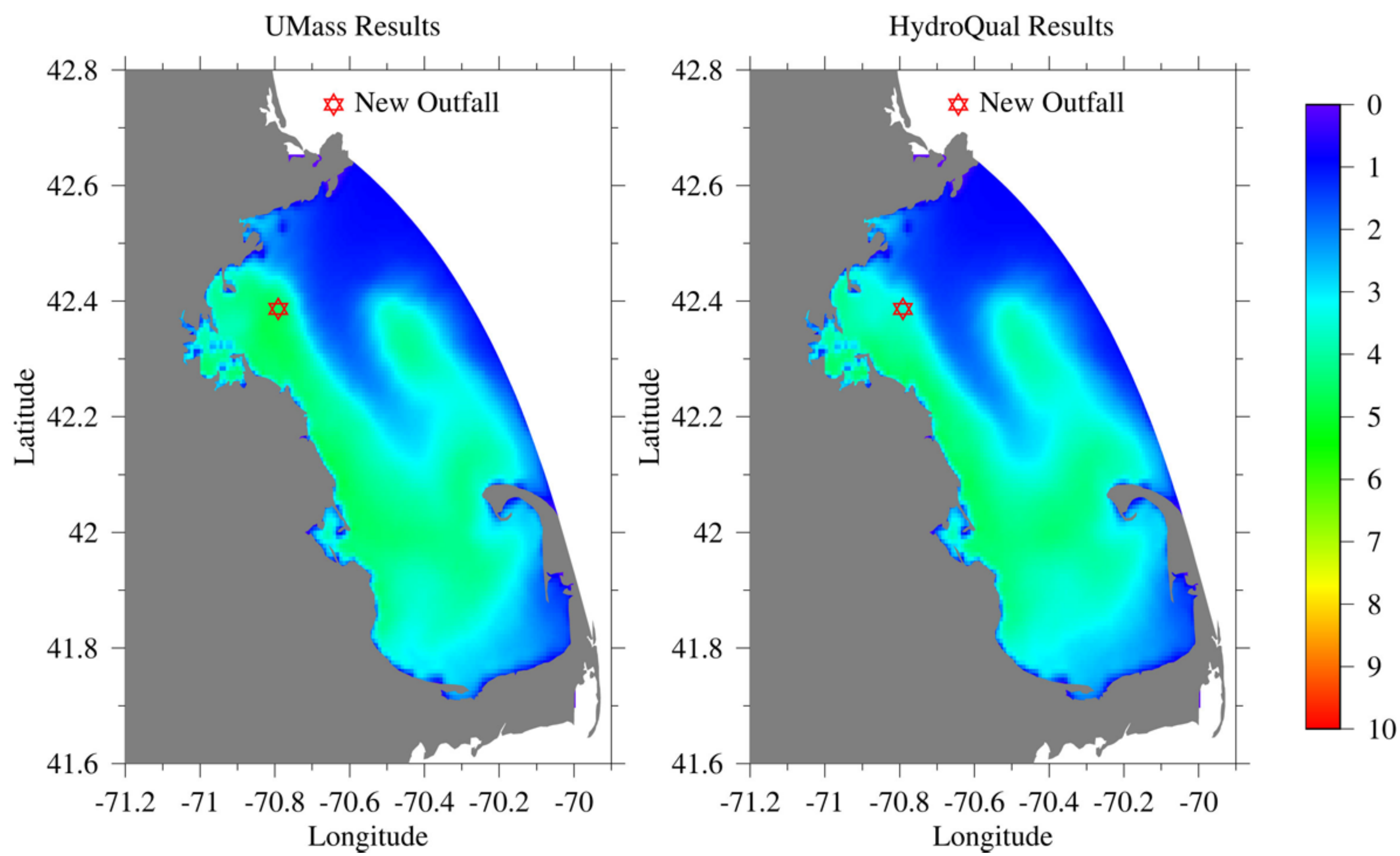

Figure 3.14. Surface Chlorophyll concentrations from April 29 to May 3.

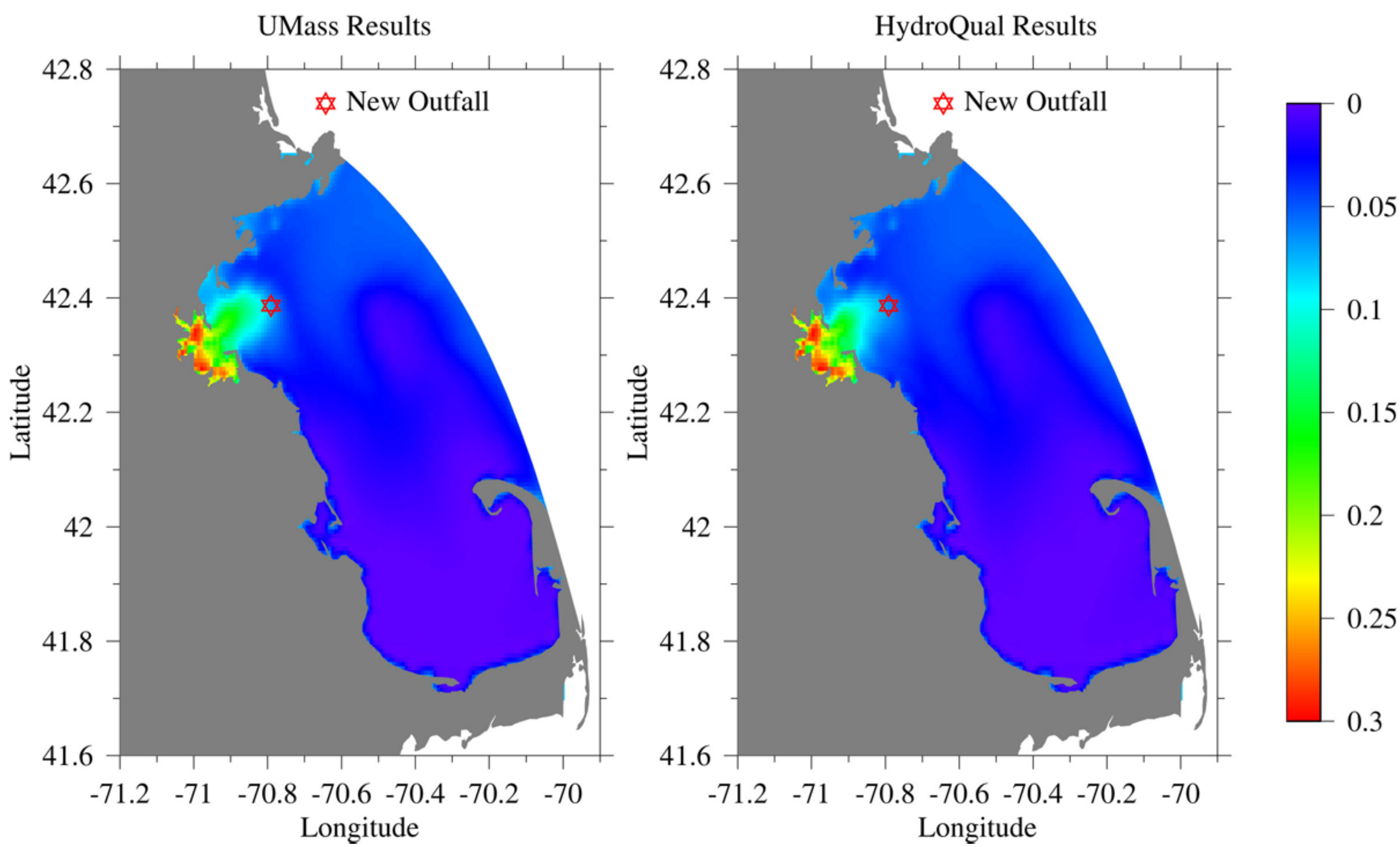

Figure 3.15. Surface DIN concentration from April 29 to May 3.

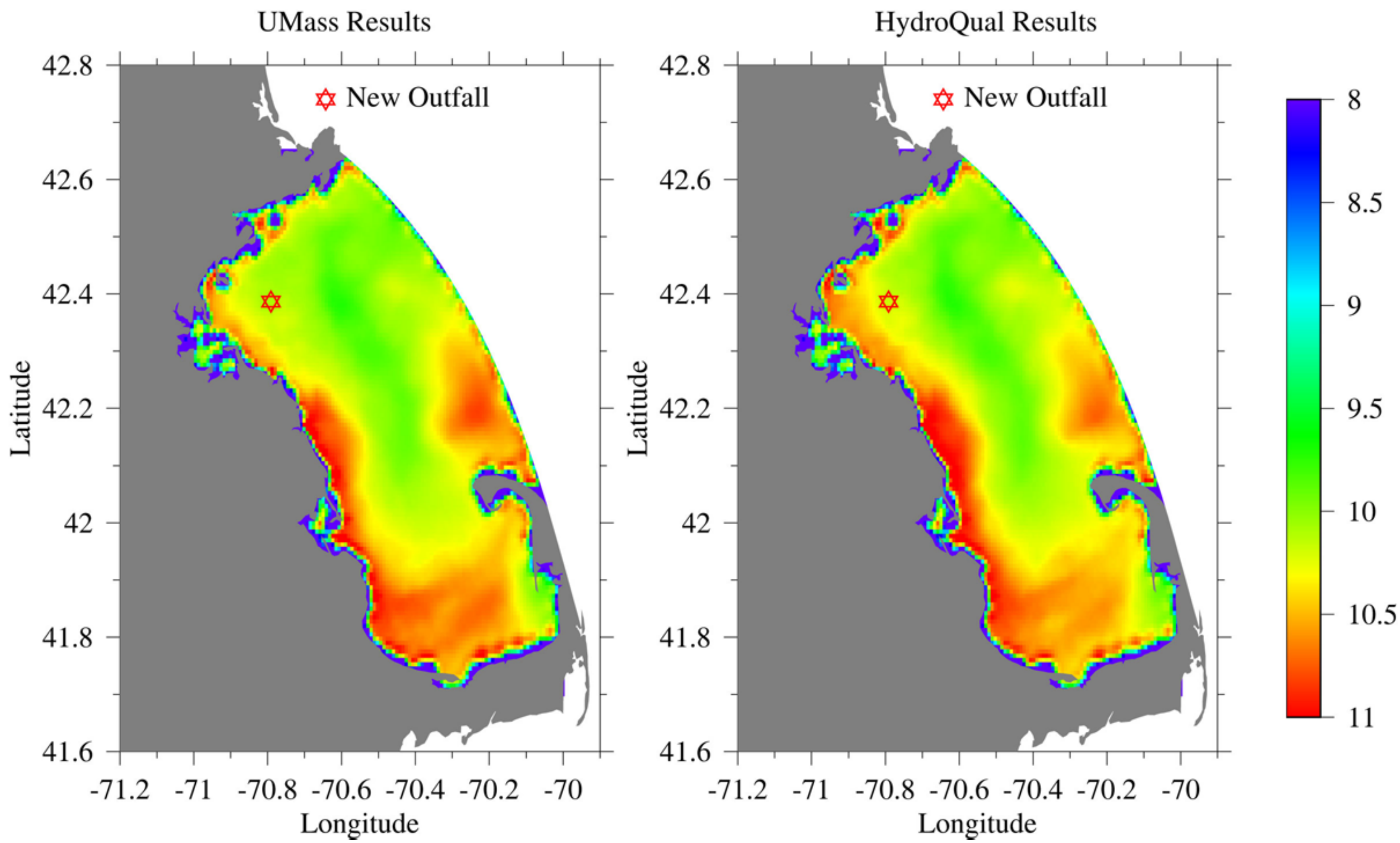

Figure 3.16. Bottom dissolved oxygen (DO) from April 29 to May 3.

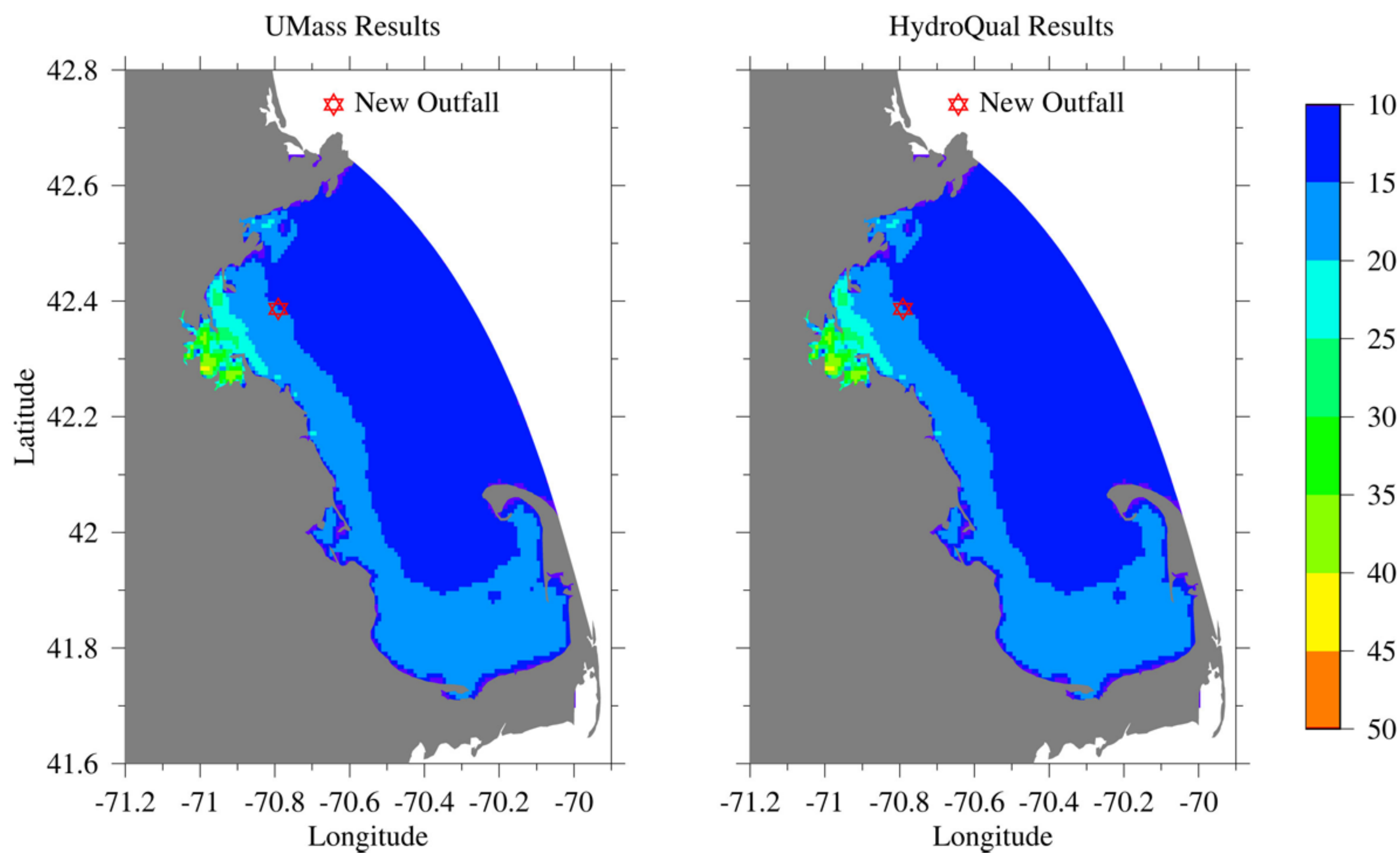

Figure 3.17. Annual mean sediment POC concentrations.

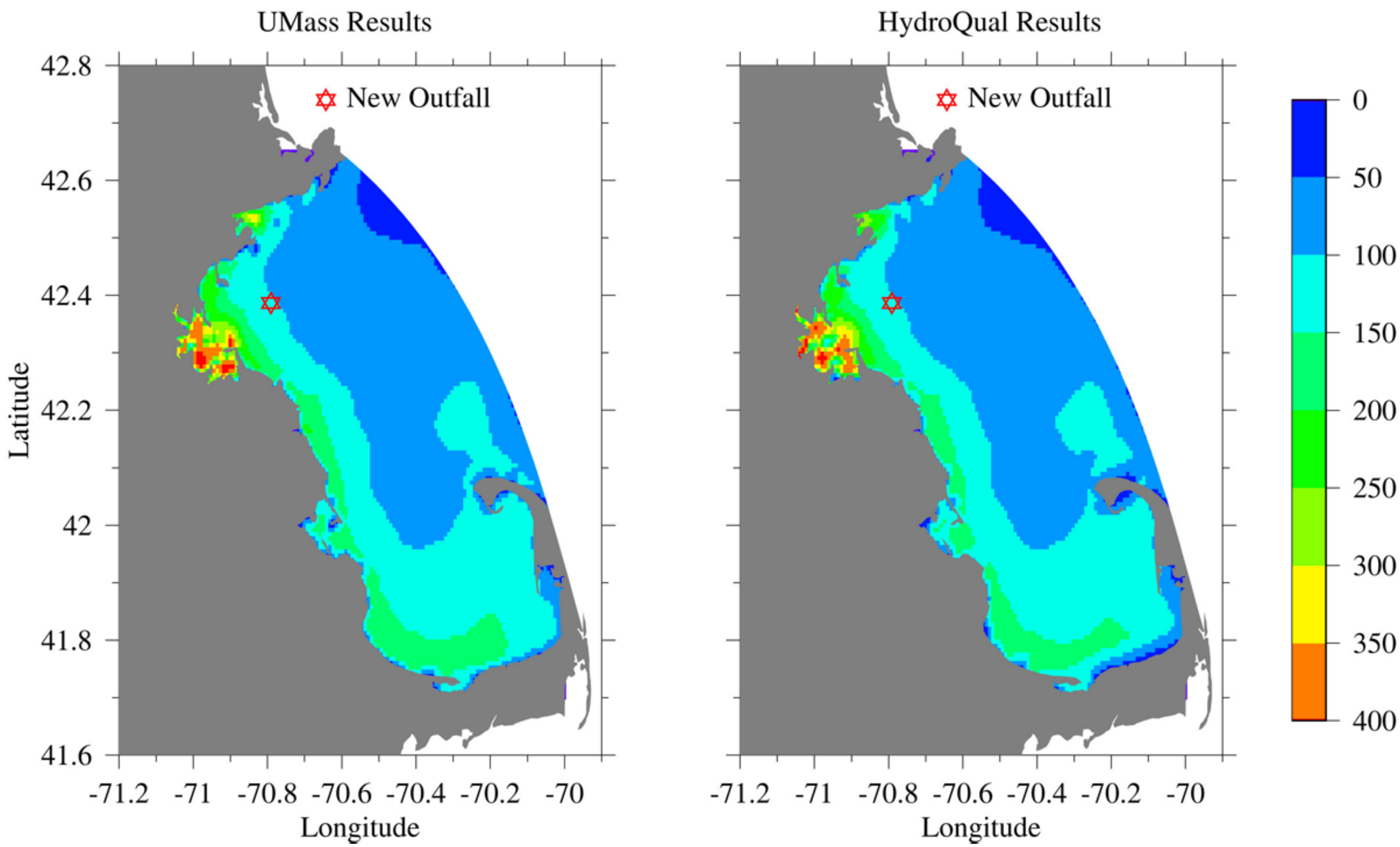

Figure 3.18. Annual mean sediment depositional flux of POC.

Section 4. Future improvements

4.1 Productivity

The HydroQual report compares the modeled primary production with observed data (Figure 4.1 in HydroQual 2001b), and indicates that the modeled primary production at Station F23 in Boston Harbor is much higher than the observed values throughout 1998, in particular, the second half of the year. Similar results were found in the second half of year 1999. By contrast, the estimates of modeled productivity at Stations N04 and N18 further into Massachusetts Bay are approximately equal to observed values. Because of limited observed data, it is unclear whether the productivity is overestimated by the model only in Boston Harbor or generally in all shallow areas. Because the chlorophyll and POC are overestimated only at Station F23 and are underestimated at all other stations during both fall 1998 and 1999, we speculate that the productivity is overestimated only in Boston Harbor.

One of the causes for the overestimation is that we used inadequate light attenuation coefficients in the model, which determines the light penetration, and in turn affect the productivity in water column. In Boston Harbor, the average water depth is approximately 4.9 m, and the maximum tidal current is approximately 50 cm s^{-1}. The turbidity produced by tidal mixing is very high from river loads and resuspension. In the model, the light attenuation is described as two parts: the geographically specific base coefficient (K_{ebase}) and the addition due to chlorophyll (K_c*Chl) where K_c is an empirical constant and Chl is the biomass of chlorophyll. K_{ebase} should theoretically include the effect of turbidity. Historic data in this region are limited. Because of the difference between observed values and model estimates of productivity, the model coefficients (K_{ebase}) used in Boston Harbor may need to be recalibrated or verified from field observations.

4.2 Fall algal blooms

The modeled fall algal blooms are much weaker in both 1998 and 1999 than the observed fall algal blooms (HydroQual, 2001b). Except nitrogen, nutrients are sufficient to support the algal growth during all seasons in both the model and observations. The modeled DIN is consistent with the observed values during the first half year, and is lower than observed values during the second half year in 1998 or 1999 (figures 5-7 and 5-12 in HydroQual, 2001b). This difference between model and observed results may indicate that the deficiency of DIN in the model results is one of the causes leading to the underestimated algal blooms in the fall.

The deficiency of DIN in the model can be caused by:

1) the DIN fluxes from the open boundary are inadequate.

2) the nitrogen recycling rate from organic pool within the water column is too low,
3) the removal rates from water column to other nutrient pools as such sediment and zooplankton are too high.

If the error is introduced at the boundary condition in case 1, the error should be diminished in areas far away from the boundary (HydroQual., 2001a). At Station F23 which is near Boston Harbor, the DIN concentration in the model is still lower than observations. Examining the cross-shelf transect of modeled DIN concentration, the strong gradient, higher in Boston Harbor and decreasing toward the offshore direction, indicates that the Boston Harbor is a major source of nutrients to the MBS. Thus, the boundary condition of DIN may not be the primary cause for the overall underestimation of fall algal blooms.

The cases 2 and 3 are associated with plankton and remineralization processes of organic matter in water column. Because the primary productivity at Station F23 is already overestimated in the model, it is most likely that the underestimation of fall blooms is caused by overestimating zooplankton grazing and removal rates to sediment, and underestimating remineralization rates in water column. A better understanding of these processes in MBS requires a detailed comparison of DON and PON between modeled and observed values that is beyond the scope of this model comparison task.

4.3 Zooplankton processes

A fixed percentage of phytoplankton standing stock (approximately 10% per day in the current simulation) is assumed to be grazed by zooplankton without involving detailed zooplankton dynamics. In ecosystem models, zooplankton processes are often simplified that zooplankton abundance follows algal blooms with a time lag. Detailed zooplankton processes are complicated by the time durations between life stages, and the time scale of their life history. The variation in the zooplankton community in the MBS adds another layer of complication. In the MBS, the zooplankton abundance increases after the spring algal bloom, reaches the maximum in late summer and early fall, and decreases in late fall and winter. A relatively low grazing rate in winter and spring and a relatively high grazing rate in summer and fall should be expected. A yearly averaged removal rate will overestimate the grazing in winter and spring and underestimate the grazing in summer and fall. However, in recent years, gelatinous zooplankton blooms in late summer and fall may have altered the zooplankton dynamics in the MBS. Their grazing on zooplankton may significantly reduce the zooplankton abundance, and reduce the grazing of zooplankton on phytoplankton in late summer and fall. A better understanding of zooplankton dynamic processes should help us to improve overall modeling results.

Acknowledgement

This work is supported by both the University of Massachusetts and Massachusetts Water Resources Authority. We would like to acknowledge Mr. Richard R. Isleib and Dr. James Fitzpatrick at HydroQual for their kind support and suggestions.

References

Bigelow, H.B., 1927. Physical oceanography of the Gulf of Maine (Part II). Bulletin of the Bureau of Fisheries, 40: 511-1027.

Blumberg, A. F. and Kantha L.H. 1985. Open boundary condition for circulation models, J. Hydraulic Engineering, 111, 273-255.

Butman, B., 1976. Hydrography and low frequency currents associated with the spring runoff in Massachusetts Bay Memoires. Societe Royale des Sciences de Liege, 6: 247-275.

Di Toro, D.M. and Fitzpatrick, J.J., 1993. Chesapeake Bay sediment flux model, HydroQual Inc., Baltimore.

Galperin, B., Kantha L.H., Hassid S. and Rosati A., 1988. A quasi-equilibrium turbulent energy model for geophysical flows. J. Atmosph. Sci., 45, 55-62.

Geyer, W.R, Gardner G.B., Brown W., Irish J., Butman B., Loder T. and Signell,R.P. 1992. Physical Oceanographic Investigation of Massachusetts and Cape Cod Bays, Technical Report MBP-92-03, Massachusetts Bays Program. U.S. EPA Region I/Massachusetts Coastal Zone Management Office, Boston. 497pp.

HydroQual, Inc., 2000. Bays Eutrophication Model (BEM): Modeling Analysis for the Period 1992 - 1994. MWRA report ENQUAD 2000-02, Massachusetts Water Resources Authority, Boston.

HydroQual., Inc., 2001a. Boundary sensitivity for the Bays Eutrophication Model (BEM). Report ENQUAD 2001-14, Massachusetts Water Resources Authority, Boston. 90p.

HydroQual, Inc., 2001b. Analysis of the addition of a third algal group to the Bays Eutrophication Model (BEM) kinetics. MWRA report ENQUAD 2001-15, Massachusetts Water Resources Authority, Boston.110p.

HydroQual, Inc., 2003. Bays Eutrophication Model (BEM): Modeling Analysis for the Period 1998 - 1999. MWRA report ENQUAD 2003-03, Massachusetts Water Resources Authority, Boston. 318p.

HydroQual, Inc. and Normandeau Assoc., Inc., 1995. A water quality model for Massachusetts and Cape Cod Bays: Calibration of the Bays Eutrophication Model (BEM). Report ENQUAD 1995-08, Massachusetts Water Resources Authority, Boston. 402p.

HydroQual, Inc. and Signell, R., 2001. Calibration of the Massachusetts and Cape Cod Bays Hydrodynamic Model: 1998-1999. MWRA reprot ENQUAD 2001-02, Massachusetts Water Resources Authority, Boston.

Large, W.G. and S. Pond, 1981. Open ocean momentum flux measurements in moderate to strong winds, J. Physical Oceanography, 11, 324-336.

Laws, E.A. and Chalup, M.S., 1990. A microalgal growth model. Journal of Limnology and Oceanography, 35: 597-608.

Libby, P.S., Albro C.S., Hunt C.D., Geyer W.R., Keller AA., Oviatt C.A. and Turner, J.T., 1999. 1998 Annual Water Column Monitoring Report. Report ENQUAD 1999-16, Massachusetts Water Resources Authority, Boston.180p.

Libby, P.S., Hunt C.D., Geyer, W.R., Keller, A.A., Oviatt C.A. and Turner, J.T., 2000. 1999 Annual Water Column Monitoring Report. Report ENQUAD 2000-09, Massachusetts Water Resources Authority, Boston. 180p.

Lynch, D.R., Naimie, C.E. and Werner, F.E., 1996. Comprehensive coastal circulation model with appliction to the Gulf of Maine. Cont. Shelf Res., 12: 37-64.

Shapiro, R., 1975. Linear filtering, Mathematics of Computation, 29, 1094-1097.

Shuter, B., 1979. A model of physiological adaptation in unicellular algae. Journal of Theoretical Biology, 78: 519-552.

Signell, R.P., Jenter, H.L. and Blumberg, A.F., 1996. Circulation and effluent dilution modeling in Massachusetts Bay: model implementation, verification and results. USGS Open File Report 96-015, U.S. Geological Survey, Woods Hole.

Werme C, Hunt C.D. 2000. 1998 Outfall monitoring overview. Boston: Massachusetts Water Resources Authority. Report ENQUAD 00-04. 66 p.

Zhou, M., 2002. Test Results of the Massachusetts Bay Hydrodynamic Model (Year 1994). ECOS 2002-2, University of Massachusetts Boston, Department of Environmental, Coastal and Ocean Sciences, Boston.

Massachusetts Water Resources Authority
Charlestown Navy Yard
100 First Avenue
Boston, MA 02129
(617) 242-6000
http://www.mwra.state.ma.us